

# Institutionen för systemteknik

## Department of Electrical Engineering

Master's Thesis

### Improved Functionality for Driveability During Gear-shift

**A Predictive Model for Boost Pressure Drop**

Master's Thesis performed in Vehicular Systems  
at The Institute of Technology at Linköping University  
by

**Mathias Brischetto**

LiTH-ISY-EX-15/4916-SE

Linköping 2015



**Linköpings universitet**  
**TEKNISKA HÖGSKOLAN**



# **Improved Functionality for Driveability During Gear-shift**

## **A Predictive Model for Boost Pressure Drop**

Master's Thesis performed in Vehicular Systems  
at The Institute of Technology at Linköping University  
by

**Mathias Brischetto**

LITH-ISY-EX-15/4916-SE

Supervisor: **Mr. Martin Sivertsson**  
ISY, Linköping University  
**Ms. Susanna Jacobsson**  
Scania, NES  
**Dr. Ola Stenlås**  
Scania, NES

Examiner: **Prof. Lars Eriksson**  
ISY, Linköping University

Linköping, 17 december 2015



	<b>Avdelning, Institution</b> Division, Department	<b>Datum</b> Date
	Vehicular Systems Department of Electrical Engineering SE-581 83 Linköping	2015-12-17

<b>Språk</b> Language <input type="checkbox"/> Svenska/Swedish <input checked="" type="checkbox"/> Engelska/English <input type="checkbox"/> _____	<b>Rapporttyp</b> Report category <input type="checkbox"/> Licentiatavhandling <input checked="" type="checkbox"/> Examensarbete <input type="checkbox"/> C-uppsats <input type="checkbox"/> D-uppsats <input type="checkbox"/> Övrig rapport <input type="checkbox"/> _____	<b>ISBN</b> _____ <b>ISRN</b> LiTH-ISY-EX-15/4916-SE <b>Serietitel och serienummer</b> <b>ISSN</b> Title of series, numbering                      _____
<b>URL för elektronisk version</b>		

<b>Titel</b> Title	Förbättrad funktionalitet för körbarhet vid växling Improved Functionality for Driveability During Gear-shift
<b>Författare</b> Author	Mathias Brischetto

<b>Sammanfattning</b> Abstract
<p>Automated gear-shifts are critical procedures for the driveline as they are demanded to work as fast and accurate as possible. The torque control of a driveline is especially important for the driver's feeling of driveability. In the case of gear-shifts and torque control in general, the boost pressure is key to achieve good response and thereby a fast gear-shift.</p> <p>An experimental study is carried out to investigate the phenomena of boost pressure drop during gear-shift and gather data for the modelling work. Results confirm the stated fact on the influence of boost pressure drop on gear-shift completion time and also indicate a clear linear dependence between initial boost pressure and the following pressure drop.</p> <p>A dynamic predictive model of the engine is developed with focus on implementation in a heavy duty truck, considering limitations computational complexity and calibration need between truck configurations. The resulting approach is based on a mean value modelling scheme that uses engine control system parameters and functions when possible. To be able to be predictive, a model for demanded torque and engine speed during the gear-shift is developed as reference inputs to the simulation. The simulation is based on a filling and emptying process throughout the engine dynamics, and yields final values of several engine variables such as boost pressure.</p> <p>The model is validated and later evaluated in comparison to measurements gathered in test vehicle experiments and in terms of robustness to input and model deviations. Computer simulations yield estimations of the boost pressure drop within acceptable limits. Considering estimations used prior to this thesis the performance is good. Input deviations and modelling inaccuracies are found to inflict significant but not devastating deviations to the model output, possibly more over time with ageing of hardware taken into account.</p> <p>Final implementation in a heavy duty truck ECU is carried out with results indicating that the current implementation of the module is relatively computationally heavy. At the time of ending the thesis it is not possible to analyse its performance further, and it is suggested that the module is optimized in terms of computational efficiency.</p>

<b>Nyckelord</b> Keywords	boost pressure, predictive, simulation, model, gear shift, automatic transmission, automated manual transmission, engine control, mean value modelling, heavy duty truck
------------------------------	--



## Abstract

Automated gear-shifts are critical procedures for the driveline as they are demanded to work as fast and accurate as possible. The torque control of a driveline is especially important for the driver's feeling of driveability. In the case of gear-shifts and torque control in general, the boost pressure is key to achieve good response and thereby a fast gear-shift.

An experimental study is carried out to investigate the phenomena of boost pressure drop during gear-shift and gather data for the modelling work. Results confirm the stated fact on the influence of boost pressure drop on gear-shift completion time and also indicate a clear linear dependence between initial boost pressure and the following pressure drop.

A dynamic predictive model of the engine is developed with focus on implementation in a heavy duty truck, considering limitations computational complexity and calibration need between truck configurations. The resulting approach is based on a mean value modelling scheme that uses engine control system parameters and functions when possible. To be able to be predictive, a model for demanded torque and engine speed during the gear-shift is developed as reference inputs to the simulation. The simulation is based on a filling and emptying process throughout the engine dynamics, and yields final values of several engine variables such as boost pressure.

The model is validated and later evaluated in comparison to measurements gathered in test vehicle experiments and in terms of robustness to input and model deviations. Computer simulations yield estimations of the boost pressure drop within acceptable limits. Considering estimations used prior to this thesis the performance is good. Input deviations and modelling inaccuracies are found to inflict significant but not devastating deviations to the model output, possibly more over time with ageing of hardware taken into account.

Final implementation in a heavy duty truck ECU is carried out with results indicating that the current implementation of the module is relatively computationally heavy. At the time of ending the thesis it is not possible to analyse its performance further, and it is suggested that the module is optimized in terms of computational efficiency.



## Acknowledgments

There are many people to whom I owe gratitude to have finished this thesis, which closes a long phase in my life.

I want to thank Scania for the opportunity to carry out a challenging but intriguing thesis project and providing supervision whenever needed. Without doubt, this project has taught me much in terms of engineering professionalism. A big thanks goes to my industrial supervisors at Scania; Ola Stenlåås, who has been of great guidance in driving the development of this thesis and Susanna Jacobson, who has supported me with her encouraging commitment to the task and guiding me in correct directions.

From the department of Vehicular Systems at Linköpings University I would like to thank my supervisor Martin Sivertsson and my examiner Lars Eriksson for their help and feedback during my thesis.

There are many more people at Scania who has supported me with technical expertise in their respective fields from the departments NESC, NESG, NECA, NECC, NMGG and others as well. A special thanks is directed to Niclas Gunnarsson and also Peter Wallebäck, who carried out the ECU implementation.

To my fellow thesis workers at NESC, I would like to direct a warm thanks for the moments and experiences we have shared together.

Finally, I want to thank my friends and family who are responsible for getting me through these five years and making them a truly joyful experience.

*Södertälje, July 2015  
Mathias Brischetto*

*“ Utan tvivel är man inte riktigt klok.. ”*

– Tage Danielsson (1928-1985)



---

# Contents

<b>Notation</b>	<b>ix</b>
<b>1 Introduction</b>	<b>1</b>
1.1 Background . . . . .	1
1.2 Objectives . . . . .	2
1.3 Delimitations . . . . .	3
1.4 Related Research . . . . .	3
1.5 Thesis Outline . . . . .	5
<b>2 Theory</b>	<b>7</b>
2.1 Automatic Gear-shifts . . . . .	7
2.1.1 Torque and Speed Control Procedure . . . . .	9
2.2 Compression Ignited Engine . . . . .	9
2.2.1 Gas Path . . . . .	10
2.2.2 Control Volumes . . . . .	11
2.2.3 Restrictions . . . . .	13
2.2.4 Intercooler . . . . .	15
2.2.5 Exhaust Gas Brake . . . . .	15
2.2.6 Turbocharger . . . . .	16
2.2.7 Waste Gate . . . . .	17
2.2.8 Combustion . . . . .	18
<b>3 Experiments</b>	<b>21</b>
3.1 Experimental Set-up . . . . .	21
3.1.1 Equipment . . . . .	22
3.2 Deviations . . . . .	22
<b>4 Modelling</b>	<b>25</b>
4.1 Modelling Considerations . . . . .	25
4.2 Development Approach . . . . .	26
4.2.1 General Structure . . . . .	26
4.2.2 Validation . . . . .	27
4.3 Reference Input Model . . . . .	27

4.3.1	Speed Profile . . . . .	28
4.3.2	Torque Profile . . . . .	28
4.4	Sub Models . . . . .	29
4.4.1	Intake Manifold . . . . .	29
4.4.2	Cylinder Air Mass Flow . . . . .	30
4.4.3	Torque Components . . . . .	30
4.4.4	Fuel Mass Flow . . . . .	33
4.4.5	Exhaust Gas Temperature . . . . .	33
4.4.6	Exhaust Manifold . . . . .	35
4.4.7	Turbocharger . . . . .	35
4.4.8	Exhaust Gas Brake . . . . .	36
4.4.9	Waste Gate . . . . .	38
4.5	Simulation Model . . . . .	39
4.5.1	Sub Model Validation and Tuning . . . . .	39
4.5.2	Simulation with Reference Input Model . . . . .	42
<b>5</b>	<b>Results and Discussion</b>	<b>45</b>
5.1	Experiments . . . . .	45
5.1.1	Impact on Total Shift Time . . . . .	46
5.1.2	Boost Pressure Drop . . . . .	47
5.2	Simulation Results . . . . .	49
5.2.1	Evaluation Method . . . . .	49
5.2.2	Model Performance . . . . .	50
5.2.3	Sensitivity to Modelling Inaccuracies . . . . .	54
5.2.4	Sensitivity to Parameter Changes and Calibration . . . . .	55
5.2.5	Sensitivity to Input Deviations . . . . .	57
5.3	Implementation in ECU for Vehicle Testing . . . . .	58
5.4	Summary . . . . .	58
<b>6</b>	<b>Conclusions</b>	<b>61</b>
	<b>Bibliography</b>	<b>63</b>

---

# Notation

## NOMENCLATURE

## SUBSCRIPTS

NOMENCLATURE		SUBSCRIPTS	
Notation	Meaning	Notation	Meaning
$A$	Area	$a, air$	Air
$c_p, c_v$	Specific Heat Capacities	$aft$	After
$D$	Diameter	$bef$	Before
$f$	Friction Factor	$c$	Compressor
$L$	Length	$cool$	Coolant
$H$	Enthalpy	$e$	Exhaust
$J$	Moment of Inertia	$eng$	Engine
$k$	Parameters	$em$	Exhaust Manifold
$M$	Torque	$f$	Fuel
$m$	Mass	$fr$	Friction
$N$	Engine Speed	$g$	Gross
$n_r$	Crank Revolutions	$ht$	Heat Transfer
$Q$	Heat Energy	$i$	Indicated (Work)
$q_{LHV}$	Fuel Heating Value	$ic$	Intercooler
$R$	Ideal Gas Constant	$ig$	Ignition
$r_c$	Compression Ratio	$im$	Intake Manifold
$T$	Temperature	$in$	Inflow
$Tq$	Torque	$inj$	Injection
$t$	Time	$m$	Mechanical
$U$	Internal Energy	$out$	Outflow
$V$	Volume	$p$	Pump
$v$	Flow Speed	$ref$	Reference
$W$	Work	$t$	Turbine
$\epsilon$	Efficiency	$tc$	Turbocharger
$\lambda$	Relative Air/Fuel Ratio	$vol$	Volumetric
$\eta$	Efficiency		
$\omega$	Rotational Speed		
$\Pi$	Pressure Ratio		
$\Psi$	Flow Velocity Function		

---

**ABBREVIATIONS**

<b>Abreviation</b>	<b>Meaning</b>
AMT	Automatic Manual Transmission
ANN	(Artificial) Neural Network
CAD	Crank Angle Degree
CAN	Controller Area Network
CI	Compression Ignited
CPU	Central Processing Unit
CVT	Continuously Variable Transmission
DCT	Dual Clutch Transmission
ECU	Engine Control Unit
EGR	Exhaust Gas Recirculation
EMS	Engine Management System
FEM	Filling & Emptying (Model)
FGT	Fixed Geometry Turbo
GMS	Gearbox Management System
MVM	Mean Value Modeling
NARMAX	Nonlinear Auto-Regressive Moving Average eXogenous
OPC	Opticruise (Scania Automatic Transmission System)
PC	Personal Computer
SCR	Selective Catalytic Reduction
SI	Spark Ignited
VGT	Variable Geometry Turbo

# 1

---

## Introduction

### 1.1 Background

A large challenge in designing a truck is the issue of driveability, which makes the driver feel comfortable and in control of the vehicle. As measure of driveability several aspects can be lifted, such as driveline oscillations and acceleration response which are both important parts of control design. Different systems in the truck need to take this design aspect into account and not least the entire driveline, which is responsible for everything regarding the propulsion. This is especially true for critical situations such as shifting gears and since automatic transmissions are widely used the responsibility of driveability lands on the automatic control systems that govern this procedure.

There is a wide selection of automatic transmissions in heavy trucks today. Some examples are; the traditional torque converter, which in effect uses a hydraulic clutch, the Continuously Variable Transmission (CVT) that allows continuous control of the gear ratio or the Automated Manual Transmission (AMT) with variations such as the Dual Clutch Transmission (DCT). The system used in Scania trucks is a type of AMT and has been the object of study in this thesis, more specifically the system developed by Scania is called Opticruise (OPC). Its transmission procedure has many similarities to the manual one governed by a human driver, but is controlled automatically by the gearbox and engine management systems (GMS and EMS) during gear-shift, hence the name AMT.

In short, gear shifts are done to keep the engine speed in a range in which it can deliver the torque demanded by the driver. When performing an automatic gear-shift, the main decision point for when and which gear to shift to, is how long the gear-shift would take at that point. That is, after engaging a new gear and closing

the clutch, how long would it take to return to the demanded torque again?

One key factor to the torque response, and not only in gear-shifting, is the state of the boost pressure. Since this pressure drops severely during gear-shifts it is of large interest to study this closer. Listed below are a number of situational parameters that could affect the boost pressure outcome. These are in several cases strongly interdependent:

- Initial boost pressure (before gear-shift).
- Engine speed during the gear-shift, directly coupled to the turbocharger speed.
- Engine torque demand.
- Current gear.
- How many steps of gear the gear box aims to shift.
- If it is an upward or downward shift.
- Fast or slow gear shifting strategy.
- Ambiental conditions.
- Time until torque can be delivered again.
- Positions of actuators, for instance intake throttle, waste gate or exhaust brake.

## 1.2 Objectives

This thesis will treat the gear-shifting procedure in heavy duty trucks with focus on the engine control aspect. More specifically the thesis aims to:

1. Develop a predictive model of the boost pressure during gear-shift.
  - The model is to be implemented in the engine control system code and incorporated into the system used today.
  - The model is to be tested in a heavy duty truck.
  - The aim of the robustness level is that it should allow to be used for different engine configurations.
  - The model functionality is to be evaluated and quantified in terms of boost pressure estimation accuracy compared to initial experiments.
  - The model robustness is to be evaluated and quantified through a sensitivity analysis.
  - The model itself is to be evaluated and quantified in terms of computational load and speed.
2. Suggest possible improvements to gear-shifts in general.
  - These improvements are to be evaluated and quantified in terms of gear-shifting speed and accuracy.

3. If time permits, possible improvements of the torque response estimation will be investigated using the new model for calculating the on-ramp.

## 1.3 Delimitations

- To reduce modelling work by limiting the width of the scope the driveline of interest has been specified with the following attributes:
  - Only fixed geometry turbochargers (FGT) will be considered since the boost pressure drop is bigger in these cases.
  - The modelling will not consider two-stage turbochargers for the same reason.
  - The engine either has no exhaust gas recirculation (EGR), which is the case for most FGT engines, or it is deactivated during gear-shifts.
- Test vehicle availability limits the choice of driveline specifications further:
  - Only transmissions using lay shaft brake will be considered. This decreases the synchronizing phase (see Section 2.1).
  - Only gear-shifts using torque controlled ramps will be considered. This increases drive comfort but could also increase down-ramping time (see Section 2.1).
- Since there are limited possibilities to run gear-shifts in test cells, the only tests will be performed in test vehicles. This has the benefit of capturing the entire driveline dynamics.
- Some external conditions that limit the possibilities are current status of for instance interfaces between the gearbox and engine control systems, CAN bus capacity for sending data and available processing power. However, suggestions that are limited by these factors would still be relevant in case of future redesign of the system, which is not unlikely.

## 1.4 Related Research

In the area of AMT modelling and control there has been much research in several aspects. Although this thesis focuses on the engine control aspect of a gear-shift some insight to the principles of AMT can be found in more general literature. Glielmo et al. [2006] treats gear-shift control strategies and gives a basic picture of an AMT process. In Pettersson and Nielsen [2000] engine controlled gear-shifts are discussed and a drive shaft torsion model is proposed in order to avoid driveline oscillations. Furthermore, since this thesis focuses on Scania's OPC, much research is found internally at Scania.

To the basic knowledge of engines both Heywood [1988] and Bosch GmbH [2007] are valuable sources, the first focuses on internal combustion while the latter

provides a wider perspective on entire automotive systems in general. Apart from the basics on engines and drivelines including AMT gear-shift operations, Eriksson and Nielsen [2014] thoroughly presents physical mean value models (MVM) of a larger part of the system.

Related to this thesis is the topic of air path and charge estimation and modelling. In Payri et al. [1999] and Galindo et al. [2014] methods of engine modelling are discussed briefly. In the latter a combination of the 0D Filling & Emptying Models (FEM) and MVM for air path modelling is chosen depending on the purpose. For transient and control oriented models where the output is represented by the boost pressure the FEM is suggested while MVM is suggested for matching calculations where, inversely, the output gives actuators positions achieving the boost pressure objective. The validity of such models is examined further in Chevalier et al. [2000] and Hendricks et al. [1996]. Extensive work in air charge estimation on a turbocharged SI-Engine has been done using the above mentioned methods in Andersson [2005]. This topic is taken further in Turin et al. [2009] where the parameters of the static physical MVM are corrected on-line using Kalman filters. Fredriksson and Egardt [2003] suggests a smoke limiting boost pressure control model but for a Diesel engine with variable geometry turbocharger (VGT), which also is the case in Guzzella and Amstutz [1998].

As an alternative to the above, data driven modelling approaches can be mentioned. These models are known as black box models and are obtained through a system identification process. Different approaches to this and modelling in general can be found in Ljung and Glad [2004]. As examples in engine modelling, Perez et al. [2006] uses Wiener-Hammerstein models and in Zito and Landau [2005] NARMAX models are used.

More advanced, also data driven, concepts are dealt with in Uzun [2014], He and Rutland [2002] and Yin and Ge [2001] where Artificial Neural Networks (ANN or just NN) are used for modelling engines. This approach is then extended with help of physical modelling in Brahma et al. [2003].

Although some of these models actually aim for low complexity, most of them are not suitable for implementation in the ECU of an EMS to perform predictive calculations. Moreover, in order to be predictive the model cannot rely on real-time updated measurements. In Darnfors and Johansson [2012], which is largely inspired by Chiara et al. [2011], a similar task for the same predictive application has been performed. This thesis, however, focuses on the boost pressure and ECU implementation of the model.

## 1.5 Thesis Outline

Here follows a description of how the thesis is structured:

**Chapter 1 - Introduction** The first chapter presents the problem to be solved and sets the scope of the thesis while also relating it to previous research in the area.

**Chapter 2 - Theory** This chapter describes the theory behind the system to give the reader a deeper understanding of the problem and lay a base to the modelling.

**Chapter 3 - Experiments** Here the experimental part of the thesis is described.

**Chapter 4 - Modelling** The modelling chapter addresses the development process of the model.

**Chapter 5 - Results and Discussion** This is where the results from experiments, model testing and implementation are presented together with a performance and sensitivity analysis of the model.

**Chapter 6 - Conclusions** The finishing chapter draws conclusions on the results and suggests directions of future work in the area.



# 2

---

## Theory

This chapter will describe the system more in detail going to give understanding for the system and thereby the objectives as well. In Section 2.1 the automated gear-shifting system and procedure is explained and in Section 2.2 theory on the compression ignited engine with models of the physical relations are presented as a base to the modelling work.

### 2.1 Automatic Gear-shifts

Gear-shifts in general are done to keep the engine in a speed range in which it can deliver the demanded torque efficiently. The transmission can either be controlled manually by the driver, or automatically by a control system, often referred to as the gearbox management system (GMS). Based on current parameters such as speed and acceleration, the GMS can decide to perform a gear-shift. These parameters serve to know when the engine would reach the limit for a suitable engine speed, referred to as *gear-shift speed*. For reference, see Figure 2.1, Graph B.

The calculation of when and how many gears to shift takes into account how long it would take to return to the demanded torque in the new gear after the gear-shift, which depends on how fast the on-ramp can be done. For different configurations of gear-shifts, i.e. how many steps and from which gear, there exists calibrated times within which the demanded torque should be reached. The gear-shift control procedure is further explained in the following sections.

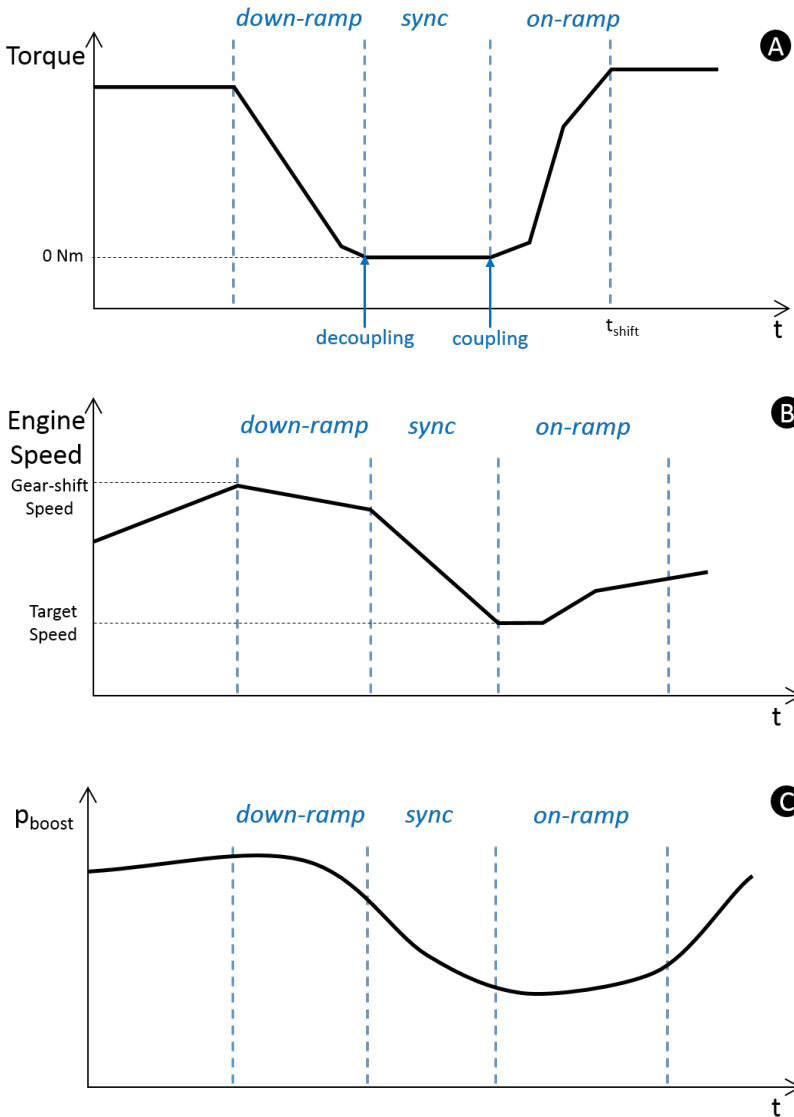


**Figure 2.1:**

A) Conceptual representation of the engine torque during an upwards gear-shift. The blue dashed lines divide the procedure into its three phases.

B) Conceptual representation of the engine speed during an upwards gear-shift starting as the engine reaches the gear-shift speed.

C) Conceptual representation of the boost pressure drop during an upwards gear-shift.

### 2.1.1 Torque and Speed Control Procedure

An AMT gear-shift is similar to the one of a manually controlled transmission. It is based on controlling the engine torque and speed whilst performing the actual changing of gears in the transmission. This procedure can be divided into three phases, which can be seen in Figure 2.1.

During the first phase the engine output torque is reduced down to zero in a *down-ramp* to allow the clutch to decouple the transmission. The ramp is designed to give a smooth and comfortable gear-shift, i.e. avoiding driveline oscillations by not dropping the fuel injection flat in one step. This is as long as the situation allows for it, as more critical situations demand faster ramps.

The *synchronization phase* starts when the clutch has been decoupled, meaning the engine and transmission speeds have to be synchronized with the speed corresponding to the new gear, called the *target speed*. For a down-shift the target speed is higher, demanding the engine to bring up the speed, whilst an up-shift requires the engine and transmission to be braked. The transmission is braked by the lay shaft brake, and the engine is braked by the exhaust brake which will be described further in Section 2.2.5.

When the new gear has been engaged and the clutch fully closed, the engine can return to deliver the torque demanded by the driver. This is done by an *on-ramp* restricted by driveline oscillations and the fact that a play in the clutch and the elasticity in the drive shafts needs to be wound up.

## 2.2 Compression Ignited Engine

Commonly used in most heavy duty trucks and several cars is the compression ignited (CI) engine. Unlike the spark ignited (SI) engine, which ignites the already mixed air and fuel with a spark, the CI combustion starts as the fuel is injected at very high pressures in the compression phase of the cylinder. Apart from this, the torque control of the CI engine is based on amount of fuel injected (see Section 2.2.8) as is not the case for the SI engine. The SI engine controls torque by regulating air flow with throttle opening. It then matches the fuel injection to keep a quite delicate balance of air to fuel ratio as an optimal trade-off between emission types. In contrast, the CI engine by necessity uses supercharging (see Section 2.2.6) to guide air into the engine only to stay above a lower limit on air to fuel ratio. This means that it normally runs on higher air to fuel ratios, which are determined by the air supply to the cylinders. The following sections will describe the most relevant topics of the CI engine gas path, with in particular, boost pressure modelling in mind.

### 2.2.1 Gas Path

Figure 2.2 shows an illustration of a turbocharged engine gas path including the air filter, compressor, intercooler, throttle, cylinder, turbine, waste gate, exhaust brake and after treatment which are all separated by pipes and manifolds.

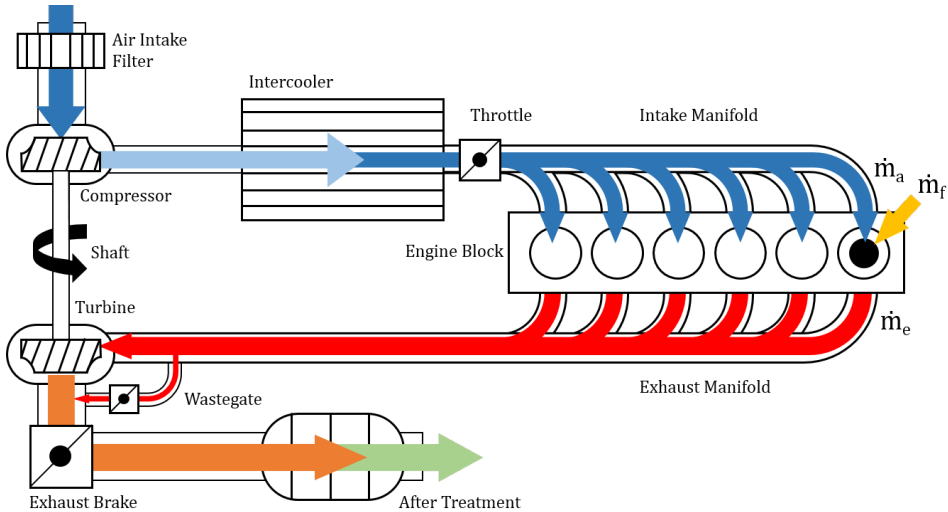


**Figure 2.2:** Figure describing the gas flow through a turbocharged CI engine. Ambient air enters through the air filter, is compressed and led through the intercooler to the intake manifold before entering the cylinder. Fuel is added in the cylinder and after combustion, the exhaust gases pass through the turbine to the after treatment system.

All components but the compressor will give induce certain pressure drops due to frictions in the air flow based on the flow rate and obstructive geometry. Components modelled after this attribute are called restrictions and they determine the passing mass flow (see Section 2.2.3). This includes the engine block that creates the pumping work in the gas path as well as the compressor and turbine. The pipes and manifolds that separate the restrictions are subject to pressure and temperature changes due to in and out mass flows and heat exchange to the environment and can be modelled as control volumes, which are explained further in Section 2.2.2. (Andersson [2005])

#### Boost Pressure

The boost pressure refers to the pressure of the air in the intake manifold right before entering the cylinders. The ideal gas law in Equation 2.1 for the intake manifold states that the boost pressure,  $p_{im}$ , is depending on the intake manifold volume,  $V_{im}$ , which is constant, the specific gas constant for air,  $R_{air}$  (neglecting humidity variations), the temperature  $T_{im}$ , and the current air mass,  $m_{im}$ , in the intake manifold.

$$p = \frac{mRT}{V} \quad (2.1)$$

The temperature and air mass depend on the ambient conditions and the turbocharger power which in turn depends on the operating points of the engine and its actuators. Further in this chapter, the components affecting the boost pressure will be explained and the physical relations presented.

## 2.2.2 Control Volumes

A thermodynamic control volume is a selected volume of a system that stores mass and energy. Figure 2.3 shows the mass and energy exchange in the form of mass and heat flows between the control volume and its environment. The energy rate balance for the volume can be stated as in Equation 2.2 where, as often done, kinetic and potential energy has been neglected.

$$\frac{dU}{dt} = \dot{W} + \dot{U}_{in} - \dot{U}_{out} - \dot{Q} \quad (2.2)$$

Here,  $E$  is the energy of the system,  $W$  denotes the total work,  $U$  internal energy and  $Q$  is the heat exchange. The work on a control volume can be divided into the work related to the pressure to introduce mass at in- and outlets (*flow work*) and all other work such as boundary displacements or shaft movements. The flow work can be expressed in terms of volume flow and pressure at the in- and outlets.

$$\dot{W} = \dot{W}_{cv} + p_{in}\dot{V}_{in} - p_{out}\dot{V}_{out} \quad (2.3)$$

Here,  $W_{cv}$  represents the other types of work. Inserting 2.3 into 2.2 and introducing the definition of enthalpy  $H$  in Equation 2.4 yields Equation 2.5.

$$H = U + pV \quad (2.4)$$

$$\frac{dU}{dt} = \dot{W}_{cv} + \dot{H}_{in} - \dot{H}_{out} - \dot{Q} \quad (2.5)$$

Now, under the assumptions of ideal gases (Equation 2.1) and that the specific heat capacities for constant volume and pressure,  $c_v$  and  $c_p$  respectively are constant, the internal energy and enthalpy can be expressed through Equations 2.6 and 2.7. A common assumption is that the volume is well-stirred so that incoming energy is instantly spread and the temperature is homogeneous throughout the volume. (Moran et al. [2011])

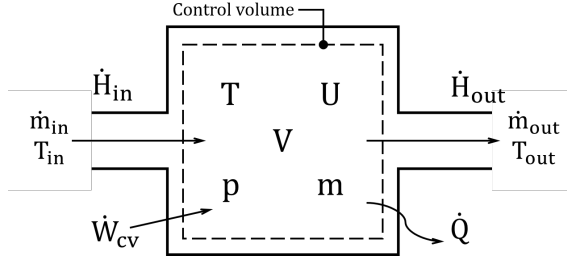


**Figure 2.3:** A control volume with exchanging energies in forms of mass flow, heat flux and work.

$$U = mc_v T \quad (2.6)$$

$$\dot{H} = \dot{m}c_p T \quad (2.7)$$

To formulate dynamic models for the piping and manifold volumes, either separately or lumped together, there are two common ways to simplify the models. The first is to assume an *isothermal* process where the temperature is constant. In this case the gas law and mass balance are sufficient to express the model since the energy conservation has been neglected to let the temperature  $T$  stay constant. The mass state is given by the difference in in- and outgoing mass flows as in Equation 2.8, which is then used in the gas law from Equation 2.1 to give the pressure state

$$\frac{dm}{dt} = \dot{m}_{in} - \dot{m}_{out} \quad (2.8)$$

$$\frac{dp}{dt} = \frac{RT}{V} \frac{dm}{dt} \quad (2.9)$$

Another, more detailed approach is to add a temperature state as a consequence of the energy exchange and in turn extend the pressure state due to the temperature change. The temperature state is essentially the differentiation of Equation 2.6 inserted in Equation 2.5 together with Equation 2.4, where the work  $\dot{W}_{cv}$  has been disregarded for these types of volumes. Furthermore, the flow work  $p\dot{V}$  has been rewritten using the gas law to fit the current choice of state variables. Differentiation of the gas law gives the pressure state. (Eriksson and Nielsen [2014])

$$\frac{dT}{dt} = \frac{1}{mc_v} \left[ \dot{m}_{in}c_v(T_{in} - T) + R(T_{in}\dot{m}_{in} - T\dot{m}_{out}) - \dot{Q} \right] \quad (2.10)$$

$$\frac{dp}{dt} = \frac{RT}{V} \frac{dm}{dt} + \frac{mR}{V} \frac{dT}{dt} \quad (2.11)$$

Apart from the temperature and pressure states  $T$  and  $p$  respectively the model is completed with the mass balance in Equation 2.8 which gives the mass state. If it is assumed that no heat exchange towards the environment occurs, the heat exchange  $\dot{Q}$  can be set to zero and the model is then called *adiabatic*.

In Chevalier et al. [2000] and Hendricks et al. [1996] the usage of MVM for engines is discussed and a study on isotherm and adiabatic models for manifolds is presented. It is clear that between the two models, the adiabatic model is more capable of following transients. However, mainly the transients in throttle tip-in and tip-outs are referred to. Since the throttle in CI engines is not used for the same purposes as in SI engines the same fast dynamic effects are not as frequently occurring. Therefore, in the case of modelling gear-shifts it is questionable how much impact the difference would have.

### 2.2.3 Restrictions

The restrictions in the system all alter the mass flow and thereby the pressure of the control volumes. These can, in terms of modelling strategy, be divided into three subgroups. For low flow speed components an incompressible turbulent flow can be assumed whilst for flows past throttling components it is common to assume a compressible flow since these flows can reach sonic conditions. The third group is application specific components that are modelled with separate approaches. (Andersson [2005])

<b>Incompressible flow restrictions</b>	{	Air filter Intercooler After treatment
<b>Compressible flow restrictions</b>	{	Intake throttle Waste gate Exhaust brake
<b>Custom restrictions</b>	{	Compressor Cylinders Turbine

Following, the incompressible and compressible flow restrictions will be explained further. The custom restrictions are explained component wise in separate sections. In Section 2.2.6 models for the turbine and compressor gas dynamics as well as the turbocharger shaft dynamics are presented. The cylinder combustion, in terms of torque and temperature models, is explained in Section 2.2.8.

#### Incompressible Flow Restrictions

Mass flow restriction models can in general be inspired from the Darcy-Weisbach Equation

$$\Delta p = f \frac{L}{D} \frac{\rho v^2}{2} \quad (2.12)$$

where  $f$  is the friction factor determined by the ruggedness of the pipe and turbulence level,  $L$  and  $D$  are length and diameter respectively. The mean flow speed  $v$  can easily be rewritten to mass flow considering pipe cross section area and fluid density and  $\rho = \frac{p}{RT}$  for ideal gases, yielding the expression for mass flow as

$$\dot{m} = \sqrt{\frac{2}{f} \frac{DA^2}{L} \frac{p}{RT}} \sqrt{\Delta p} = C \sqrt{\frac{p}{T}} \sqrt{\Delta p} \quad (2.13)$$

where alternatively the parameter  $C$  can be determined through a least square method given measurement data.

### Compressible Flow Restrictions

Compressible flow restrictions like throttles are usually modelled by standard orifice equations from Heywood [1988]

$$\dot{m} = \frac{p_{bef}}{\sqrt{RT_{bef}}} A_{eff} \Psi(\Pi), \quad \Pi = \frac{p_{aft}}{p_{bef}} \quad (2.14)$$

where  $A_{eff}$  is the effective orifice open area that for practical modelling reasons is the actual open area lumped together with the discharge coefficient which depends on the orifice geometry as in Eriksson and Nielsen [2014].  $\Pi$  is the pressure ratio across the valve, depending on which, one of two definitions for  $\Psi$  is used. The critical pressure ratio at which the flow through the orifice reaches sonic velocity is defined as

$$\Pi_{cr} = \left( \frac{2}{\gamma + 1} \right)^{\frac{\gamma}{\gamma - 1}} \quad (2.15)$$

where  $\gamma$  is the heat capacity ratio. To determine  $\Psi$  for sub critical flows Equation 2.16 is used, otherwise if the flow is choked, Equation 2.17 is used.

$$\Psi = \sqrt{\frac{2\gamma}{\gamma - 1} \left( \Pi^{\frac{2}{\gamma}} - \Pi^{\frac{\gamma+1}{\gamma}} \right)} \quad (2.16)$$

$$\Psi = \sqrt{\gamma \left( \frac{2}{\gamma + 1} \right)^{\frac{\gamma+1}{\gamma-1}}} \quad (2.17)$$

### 2.2.4 Intercooler

The intercooler aims to reduce the intake air temperature and is designed to exchange as much heat as possible. It thereby fills several purposes; one is to increase the air density so that more oxygen can enter the combustion chamber, another is that with lower combustion temperatures comes lower NO<sub>x</sub>-emissions. (Heywood [1988]).

The pressure drop in the intercooler is suitable to model as an incompressible flow restriction as presented in Equation 2.12. To take into account the temperature drop that is likely to occur under most operating conditions a model for heat exchangers can be included. The heat exchanger can then be assumed to be of type cross flow with both fluids unmixed, which is the case for most commonly used intercoolers. Since the larger temperature drop is in the fluid with lowest air mass flow, the model uses the ratio between the temperature differences between incoming air, and outgoing air and coolant air as measure of effectiveness. This yields Equation 2.19 as the outgoing temperature.

$$\epsilon = \frac{T_c - T_{ic}}{T_c - T_{cool}} \quad (2.18)$$

$$T_{ic} = T_c - \epsilon(T_c - T_{cool}) \quad (2.19)$$

where incoming air  $T_c$  is the compressor outgoing temperature,  $T_{ic}$  is the outgoing intercooler temperature and  $T_{cool}$  is the coolant air temperature, which normally is the ambient temperature. (Brugård [1999])

### 2.2.5 Exhaust Gas Brake

The exhaust brake consists of a throttling mechanism that is placed after the turbine. The main use is to brake the engine by closing the valve and building up back-pressure in the exhaust manifold and thereby increasing the pumping work. These effects can be used in other purposes as well, as for instance to heat exhaust gases to hurry the heating of the catalyst or to limit the white smoke generation. However, since exhaust gases are slowed down the turbocharger speed is directly affected.

The exhaust brake could be modelled as a compressible turbulent restriction since it has the basic properties of a throttle. Some aspects should however be taken into account. The throttle plate is placed eccentrically on a shaft to enable a self-opening feature and the shaft is connected to an arm controlled by a pneumatic proportional valve with a counteracting spring. Some characteristics concerning the pneumatic system is for instance the delay in actuation and some hysteresis in the proportional valve and the actuator, mainly due to the eccentricity of the axle. Furthermore, there is a possibility for an individual spread amongst proportional valves.

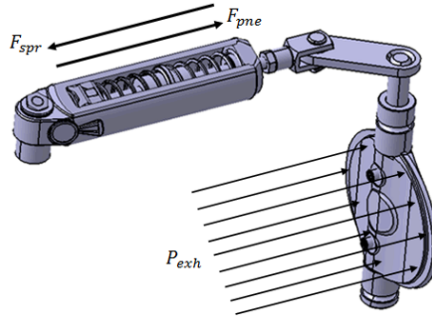


Figure 2.4: The exhaust gas brake mechanism.

## 2.2.6 Turbocharger

Used in most heavy duty trucks is some kind of supercharging method for increasing the intake air density. By doing this, the engine can be designed to be smaller (downsizing) without sacrificing the power output, thus resulting in better fuel economy. One of the more common ways is to use a turbocharger where a turbine propelled by the exhaust gas flow, through a shaft mechanically drives a compressor placed at the air intake. (Eriksson and Nielsen [2014])

The turbocharger speed dynamics can be described as a power balance between compressor and turbine. These are modelled separately and connected through the shaft model based on Newton's second law of motion in Equation 2.20. The turbocharger speed dynamics  $\omega_{tc}$  is here subject to the turbine power input  $\frac{d\omega_{tc}}{dt}$  and compressor power outtake  $\dot{W}_c$ .

$$\frac{d\omega_{tc}}{dt} = \frac{1}{J_{tc}} \left( \frac{\dot{W}_t}{\omega_{tc}} \eta_m - \frac{\dot{W}_c}{\omega_{tc}} \right) \quad (2.20)$$

Where  $J_{tc}$  is the turbocharger inertia and  $\eta_m$  the mechanical inefficiency causing a power loss at the power input. Both compressor and turbine characteristics are usually determined experimentally to build models based on relations of pressure ratios, mass flows and temperatures. Equations 2.21 and 2.22 are the resulting generic models of mass flow  $\dot{m}$  and efficiency  $\eta$  of compressor and turbine, which often are expressed as maps.

$$\dot{m} = f_{\dot{m}}(p_{bef}, p_{aft}, T_{bef}, \omega_{tc}) \quad (2.21)$$

$$\eta = (p_{bef}, p_{aft}, T_{bef}, \omega_{tc}) \quad (2.22)$$

Where  $\omega_{tc}$  is the turbocharger angular speed and indices *bef* and *aft* denote a

quantity before and after the component respectively. Furthermore, Equation 2.5 for a control volume together with Equation 2.7 are suitable to express the powers for compressor and turbine. The assumption of steady state flow without heat transfer in the components control volumes ( $\frac{dE}{dt} = 0$  and  $\dot{m}_{in} = \dot{m}_{out}$ ) yields Equations 2.24 and 2.23.

$$\dot{W}_c = \dot{m}_c c_{p,c} (T_c - T_{air}) \quad (2.23)$$

$$\dot{W}_t = \dot{m}_t c_{p,c} (T_{em} - T_t) \quad (2.24)$$

where  $T_c$  is the temperature after the compressor,  $T_{air}$  is the incoming air temperature,  $T_{em}$  is the exhaust manifold temperature and  $T_t$  is the temperature after the turbine. The temperature after the component is found by assuming that an ideal process is isentropic and expressing the inefficiency with a factor  $\eta_c$  for the compressor and  $\eta_t$  for the turbine.

$$\left\{ \begin{array}{l} \eta_c = \frac{\dot{W}_{c,ideal}}{\dot{W}_{c,actual}} \\ T_c = T_{air} + \frac{T_{air}}{\eta_c} \left\{ \left( \frac{p_c}{p_{air}} \right)^{\frac{\gamma-1}{\gamma}} - 1 \right\} \end{array} \right. \quad (2.25)$$

$$\left\{ \begin{array}{l} \eta_t = \frac{\dot{W}_{t,actual}}{\dot{W}_{t,ideal}} \\ T_t = T_{em} - \eta_t T_{em} \left\{ 1 - \left( \frac{p_t}{p_{em}} \right)^{\frac{\gamma-1}{\gamma}} \right\} \end{array} \right. \quad (2.26)$$

Here  $\gamma$  is the heat capacity ratio  $\frac{c_p}{c_v}$  for air and exhaust gas respectively. However, as turbines often operate at high temperatures that cause heat transfer, using the assumption of no heat transfer could cause the efficiency to be overestimated. To remedy this it is possible to express the turbine efficiency in terms of compressor work and mechanical efficiency  $\eta_m$  as follows.

$$\eta_t = \frac{\dot{W}_c / \eta_m}{\dot{W}_{t,ideal}} \quad (2.27)$$

## 2.2.7 Waste Gate

For turbochargers with fixed geometry (FGT) the turbine power can be controlled by the waste gate that bypasses a certain amount of the exhaust gases past the turbine. By controlling the opening of the valve, the turbocharger speed and in turn the boost pressure can be controlled. For high loads it will also protect the turbocharger from over-speeding. In cases necessary, the waste gate can be modelled using the before mentioned Equation 2.14 for orifices.

### 2.2.8 Combustion

The exhaust gas flow in a diesel engine involves both fuel injection  $\dot{m}_f$  and mass flow from the intake manifold  $\dot{m}_{im}$ . Naturally, the exhaust output  $\dot{m}_e$  is a sum of both as seen in Equation 2.28. The demanded torque (Equation 2.31), engine operating efficiency and fuel heating value determine what amount of fuel to inject, while the amount of air depends on the intake manifold conditions, engine volumetric efficiency and EGR-fraction as seen in Equation 2.30. The amount can also be adjusted by controlling the valve opening time and lift.

$$\dot{m}_e = \dot{m}_f + \dot{m}_{im} \quad (2.28)$$

The ratio between air and fuel in the engine is expressed in terms of relative air/fuel ratio  $\lambda$ . Using a lambda sensor that measures relative oxygen levels in the exhaust gases, the air/fuel ratio can be calculated according to Equation 2.29. In CI engines the lambda sensor is usually only used for diagnostic purposes and is placed in the after treatment system.

$$\lambda = \frac{m_a}{m_f(A/F)_s} \quad (2.29)$$

#### Air Flow

The mass flow into the cylinder is the same as the flow out of the intake manifold and is proportional to the intake pressure, volumetric efficiency  $\eta_{vol}$  and inversely proportional to the intake temperature. If EGR is not used the mass flow can be assumed to be only air, otherwise the EGR-fraction must be included.

$$m_{im} = m_a + m_{egr} = \eta_{vol} \left( N, p_{im}, p_{em}, r_c, T_{eng} \right) \frac{p_{im} V_c}{RT_{im}} \quad (2.30)$$

Where  $V_c$  is the cylinder volume and  $\eta_{vol}$  describes the engine's effectiveness in taking in new air into the cylinder. The volumetric efficiency depends on several engine parameters such as engine speed  $N$ , intake and exhaust manifold pressure  $p_{im/em}$ , compression ratio  $r_c$  and engine temperature  $T_{eng}$ . Either models of the volumetric efficiency derive from these physical relations or go more towards black box approaches. (Eriksson and Nielsen [2014], Hendricks et al. [1996], Jensen et al. [1991])

#### Torque Components

The total torque demand needs to cover the demanded output to the flywheel, the torque consumed by auxiliary systems and inefficiencies of the combustion engine. The main components in the cylinder work are, except from the produced gross indicated work  $W_{i,g}$ , the coolant losses  $W_{i,c}$ , pumping losses  $W_{i,p}$  and friction losses  $W_{f,r}$ . If  $M_e$  is the engine torque output, its equation yields:

$$M_e = \frac{W_e}{n_r 2\pi} = \frac{W_{i,g} - W_{i,p} - W_{fr} - W_{i,c}}{n_r 2\pi} \quad (2.31)$$

Where  $n_r$  is the number of crank revolutions in a complete four-stroke power generation cycle. The gross indicated work is a function of injected fuel mass, fuel heating value  $q_{LHV}$  and a factor of operating efficiency  $\tilde{\eta}_{ig}$  that lumps together different loss factors like; losses in the ideal thermodynamic cycle  $\eta_{f,ig}$ , suboptimal injection crank angle degree (CAD) timing  $\eta_{ig}(\alpha_{inj})$ , remaining unburnt fuel in the exhaust gases (mostly for rich mixtures  $\lambda$ ) and combustion chamber heat losses  $\eta_{ig,ch}$  according to the following equation:

$$W_{i,g} = m_f q_{LHV} \tilde{\eta}_{ig} \left( \eta_{f,ig}, \eta_{ig}(\alpha_{inj}), \lambda, \eta_{ig,ch} \right) \quad (2.32)$$

## Temperature

The engine outgoing temperature  $T_e$  is what remains of the input energy in the exhaust gases after combustion. Therefore, one way to model the temperature is to find out how much energy is input to the cylinder and how much does not exit the cylinder through the exhaust gases. This can be modelled through the first law of thermodynamics by summing the energy flows of the combustion components as in the following equation:

$$\dot{m}_e c_p (T_e - T_{im}) = \dot{Q}_f - \dot{W}_{i,g} - \dot{Q}_{ht} \quad (2.33)$$

where the left hand side lumps together the added temperature energy of the incoming air and fuel masses and  $c_p$  is the specific heat capacity, which is assumed to be constant and the same as for air. Here  $T_{im}$  is the air and fuel temperature (assuming the fuel has the same temperature as the air).  $\dot{Q}_f$  is the chemical energy of the fuel:

$$\dot{Q}_f = \dot{m}_f q_{LHV} \eta_\lambda \quad (2.34)$$

where  $q_{LHV}$  is the lower heating value of the fuel and  $\eta_\lambda$  an efficiency factor caused by the inability to completely burn too rich mixtures.  $\dot{W}_{i,g}$  is the work produced on the piston already explained in Equation 2.32.  $\dot{Q}_{ht}$  constitute the heat transfer to the coolant system through the cylinder walls and must be derived from experimental data. However, another approach adopted from Tschanz et al. [2013] is shown in Equation 2.35, where the part of the heat produced exiting with the exhaust gases is approximated by a function of engine speed  $N$  and injected fuel  $\dot{m}_f$ .

$$\begin{cases} \dot{m}_e c_p (T_e - T_{im}) = k_T (\dot{Q}_f - \dot{W}_{i,g}) \\ k_T = k_e + k_N (N - N_{ref}) + k_f (\dot{m}_f - \dot{m}_{f,ref}) \end{cases} \quad (2.35)$$

Here the function  $k_T$  has the parameters  $k_e$ ,  $k_N$  and  $k_f$  that need to be determined through a least square estimation.

# 3

---

## Experiments

This chapter describes how the experiments were set up and performed to yield useful results. The main goal of the experiments was to carry out realistic and repeatable situations while gathering data for statistical examination and signals for validation during model development.

### 3.1 Experimental Set-up

Limited by the layout and topology of the Scania test course the below listed situational variations while gear shifting were sought. However, focus was on inducing the more critical gear-shifting situations under tougher loads.

- Shifts upwards and downwards
- Shifts of different number of steps
- At different accelerator pedal positions
- At different speeds/gear numbers
- Gear-shifting strategies of varying aggressiveness
- Different loads: uphill/downhill, different truck combination or while using retarder
- Accelerating from low boost pressure: Starting from stand still or low accelerator pedal position.
- If possible, induce failed gear-shifts.

In order to conduct rewarding and repeatable experiments a few scenarios were constructed. The scenarios are formulated in Table 3.1 below with first the action and then what effects were tried to reach. Hills 1-4 are denotations of specific hills in the Scania test course.

*Table 3.1: Examples of constructed scenarios*

<b>Action</b>	<b>Outcome</b>
Hill 1 at ~30km/h	Fast gear changes
Start in Hill 1	Shifting smaller steps Low boost pressure
Hill 2 at ~40km/h	Part Load Down gear-shifts
Start in Hill 3 (Tough)	Low boost pressure Fast gear changes
Start downhill before Hill 3	High gear coming into tough hill Fast gear changes
Rolling down Hill 4, ~60km/h, Full gas when flattening	Shifting multiple steps Low boost pressure
Starting at flat, full gas	Normal gear-shifts Low boost pressure

### 3.1.1 Equipment

- Specified EMS/GMS Software Versions (continuously used)
- Logging equipment for both engine and gearbox
- 10Hz Sampling time
- Specifications of used trucks follow in Table 3.2

## 3.2 Deviations

The outcomes of the tests are presented as results in Section 5.1. There the particular results are plotted and discussed. On the test performance some remarks can be lifted:

- For different truck configurations, particularly weight/power ratio, the scenarios produce different effects, which make them more or less suitable for one truck or the other. This mainly affected the ability to induce situations with tougher load for the lighter truck, which lead to more frequent retarder use.

**Table 3.2: Truck specifications**

<b>Name</b>	<b>Clint</b>	<b>Bolsena</b>
Type	Hauler	Distribution
Weight	~39 Tonnes	~11 Tonnes
Engine Size/Power	6-cyl /450hk	5-cyl /280hk
Turbo/AT	FGT/SCR	FGT/SCR
Transmission	OPC, 2-pedal	OPC, 2-pedal
	Layshaft Brake	Layshaft Brake

- In general, down-shifts occur more seldom but with larger downward gear steps, which lead to fewer down-shift recordings.
- The experiments were performed during several occasions at which new measurements and logged signals were added since the progressing modelling work introduced further investigation objectives.



# 4

---

## Modelling

This chapter addresses the model development and validation process. It is presented what approaches have been used and the different parts of the model are described.

### 4.1 Modelling Considerations

To model the system there are several approaches to choose between. These vary in the range between black and white box modelling. A white box model would completely rely on physical relations to explain the behaviour of the system, while a black box model would use a suitably parametrized mathematical structure to explain the unknown relation between inputs and output. (Ljung and Glad [2004])

The latter is preferable for complex non-linear systems with unknown physical relations, while a simpler system could be modelled using a physical description. In the middle case it is usual to combine these approaches by adding parameters that can be fitted to account for simplifications in the physical models, these are sometimes referred to as grey box models.

Listed below are some aspects of the system that restrict the modelling approach.

**Predictability:** The model needs to be able to foresee the boost pressure during gear-shift. This means that for an initial operating point and a following series of given engine reference signals the model should simulate the remaining parameters. Compared to a real-time simulated system, engine parameters cannot be updated to continuously updated measurements.

**Low complexity:** To let the simulation be updated at a satisfactory frequency

and not taking up too much CPU capacity in the ECU the model complexity should for an acceptable accuracy level be kept low. If possible, already implemented code in the control system should be used.

**Robustness:** Since the model should be valid for several engine configurations the model should gather available parameter data from the system in cases where it is possible. Otherwise, these parameters have to be calculated beforehand or on-line during operation by the system itself.

## 4.2 Development Approach

The approach is to model the engine so that the boost pressure during a gear-shift can be simulated and extracted at the desired point in time. For this a physical MVM is a suitable initial approach as a large part of the engine can be explained with known relations that uses averaged values over several engine cycles and neglects in-cycle variations, these are well covered in Eriksson and Nielsen [2014] and Andersson [2005]. Furthermore, the engine control system already contains functions and mapped data for calculating physical relations and can be used in order to reduce calculation complexity, simplify models and make the model easier to apply to a wider selection of engine configurations.

### 4.2.1 General Structure

The entire developed model consists of the two parts presented in Figure 4.1. The first part simulates the gear-shift reference conditions, which are then used as inputs to the second part that simulates the engine during the gear-shift and outputs the boost pressure, further on referred to as the simulation model.

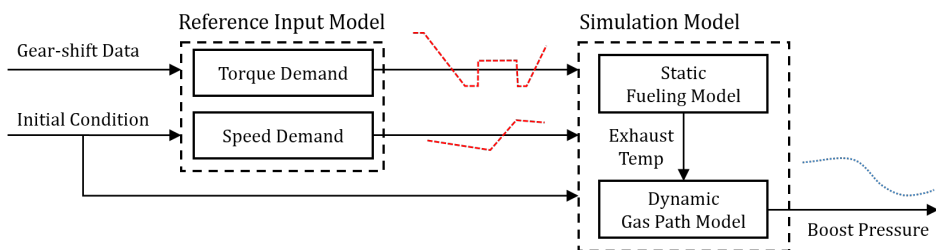


*Figure 4.1: Reference input model and simulation model overview.*

As gear-shifts are controlled by predefined sets of calibrated instructions for each gear-shift type, these are used to model the reference inputs to the simulation model. The instruction parameters are determined by current driving conditions that can be gathered from sensors or EMS-signals, which is explained further in Section 4.3. Furthermore, the current states of signals and sensors are also used as initial conditions for the simulation model.

## 4.2.2 Validation

To validate models, the EMS-signals logged during the experiments are used. This is considered as a limitation in both modelling and validation since these measurements are less accurate than in test cells. These are also in some cases not actual sensors but virtual sensors modelled in the EMS code.

Static sub models are calibrated and validated against either scatter plots or time based plots using other EMS-signals as inputs. In the validation time plots presented in Section 4.4, a signal to indicate when gear-shifts occur is included as a binary value, normalized to the other plotted parameters. This signal activates just as the down-ramp starts and returns to zero as the clutch is re-engaged.

After validating these models individually they are plugged into the dynamic relations to simulate the gear-shifts. In order to qualitatively assess the performance of the simulation, a number of time segments with individual gear-shifts are manually selected from the experiments. By comparing sensor signals to the modelled signals, conclusions on the performance can be made to find weaknesses in the model structure and parameter choices.

Initially, the logged signals for demanded torque and engine speed are used as reference inputs. This ensures that the physical relations described in the models are properly tested since modelling errors in the reference signals can be ruled out, these are explained further in Section 4.3. At this stage parameter tuning is done to fit the simulation model to the system behaviour, which is addressed in detail in Section 4.5.

## 4.3 Reference Input Model

To simulate the process, the model only needs initial conditions, demanded torque output and engine speed. Since the model needs to be predictive it can only use information known prior to the gear-shift and from that build reference signals of torque and engine speed. This approach has much in common with the one used in Chiara et al. [2011], which inspires the schematic overview of the model principle presented in Figure 4.1.

Considering the decision process for gear-shifting, there are two possible approaches to acquire information to model the reference inputs for a certain gear-shift. Either the model receives finally decided ramping and syncing strategies that would be sent on the CAN-bus, or it makes use of calibration data and imitates the actual ramp calculations. Here the latter approach has been chosen in order to avoid CAN-traffic that requires design of a new interface for the price of possible modelling inaccuracy.

Furthermore, since the decision of which gear to choose, i.e. how many steps to shift, is to be based on the outcome of this model a paradox of which target speed to simulate for appears. To break this circular dependence, reference profiles of five target speeds are modelled. Out of the results it is then possible to interpolate

a final boost pressure for any target speed, on which the gear-shift decision can be based.

### 4.3.1 Speed Profile

During the down ramping the speed can either be assumed to stay constant or keep constant acceleration. In case of noise in the speed signal it is not suitable to use differentiation unless the signal is averaged over several points. The speed is therefore set constant. Since the final speed  $N_{target}$  is assumed to be known for a certain gear-shift and the acceleration is assumed constant Newton's second law of motion yields the relation in Equation 4.1.

$$M_e = J_{eng} \left( \frac{N_{target} - N_{actual}}{t_{sync}} \right) \quad (4.1)$$

Where  $J_{eng}$  is the moment of inertia of the decoupled engine. Here the torque could be known if the shifting strategy were known. Since this implementation assumes it is not, the sync time must be assumed to be known and is set as a tuning parameter. Examinations of recorded gear-shifts show that sync times keep within certain limits, with a few exceptions. This yields the speed profile of the ramp. The speed after reaching the target speed can be assumed constant or to resume to the previously held acceleration. For evaluation, the five speed reference profiles are plotted against the real speed with the same initial conditions as the simulations are intended to run. Out of several tested gear-shifts, two are plotted in Figure 4.2 next to their respective torque profile.

### 4.3.2 Torque Profile

Starting at the initial condition the torque needs to be ramped down to zero. The ramp derivative is calibrated for individual truck configurations and adapted to situational parameters. In the model this calibrated data is used together with situational factors such as pedal position and current gear.

At the sync phase, a certain torque will be demanded in order to ramp the engine to the target speed, either positive torque or brake torque translated into exhaust gas brake actuation for down-shifts and up-shifts respectively. This depends on how fast the gear-shift needs to be performed. As previously mentioned, the sync torque is not known in this implementation, which means it has to be calculated according to Equation 4.1 given the speed profile.

Up-shifts require that no fuel is injected during sync and ideally that the exhaust gas brake is activated at a level corresponding to the negative torque demand, which is not known in this implementation. Ultimately, this means that the same approach as used for the down-shifts could be viable for up-shifts as well. For evaluation of the torque profiles, see Figure 4.2 where two examples are shown next to the corresponding speed profile. Here the negative torque demands would represent up-shifts.

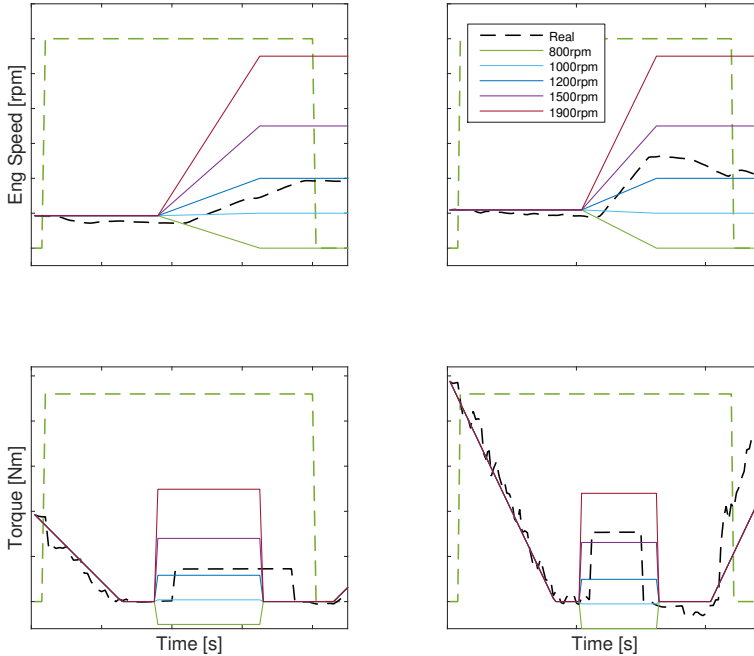


**Figure 4.2:** Reference input model examples for two different down-shifts, where the coloured and solid lines represent the modelled torque (lower) and speed reference inputs (upper) for each of the five engine speeds.

## 4.4 Sub Models

The simulation model is constituted by several sub models of control volumes and restrictions as described in the theory in Chapter 2.2. An overview of the sub model structure is presented in Figure 4.3, where the dynamic sub models receive their initial conditions when starting the simulation. The following sections address the different sub models in respect to their modelling strategy, final structure and validation process.

### 4.4.1 Intake Manifold

At the core of the model, the intake manifold is modelled as an isothermal control volume with filling and emptying dynamics according to equations 2.8 and 2.9, where the temperature is assumed to stay constant during the simulation. This assumption is helped by the fact that the intercooler is able to smooth out temperature fluctuations in the compressor outflow. The compressor air mass flow gives the in flow and the cylinder air mass flow sets the out flow, while the current state

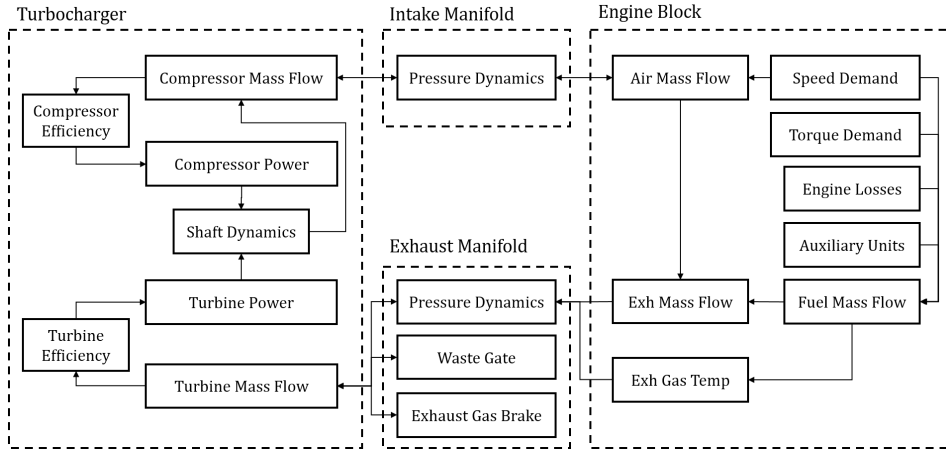


**Figure 4.3:** Sub model structure overview, where arrows indicate main dependencies.

in the intake manifold sets the conditions for both models to operate from. At the end of the gear-shift simulation, this model yields the final boost pressure.

#### 4.4.2 Cylinder Air Mass Flow

Using Equation 2.30, the air mass flow into the cylinder and out of the intake manifold can be calculated. For the volumetric efficiency  $\eta_{vol}$  a static look-up table for engine speed dependency is used. This look-up table uses EMS-specific calibrated data.

The air mass flow sub model is validated against an EMS-model signal based on intake manifold pressure measurements. Since the models are identical, the only discrepancy lies in volumetric efficiency. The existing EMS-function uses a look-up table with correction based on load and pressure ratios. A simpler method is to use only the basic look-up table. Although these in most cases produce similar results, there is a large difference for exhaust gas braking where exhaust back pressure peaks. The validation plot is shown in Figure 4.4, in which the final model using the map follows well even though there is a difference in volumetric efficiency.

#### 4.4.3 Torque Components

The torque model is based on Equation 2.31, where the left hand side is the demanded output. To calculate the specific losses, mapped data available in the EMS to match fuel injection to total torque consumption is used. Here, variables such as engine speed, engine temperature, boost pressure and exhaust pressure, which are all available in the simulation model, are inputs to the static maps.

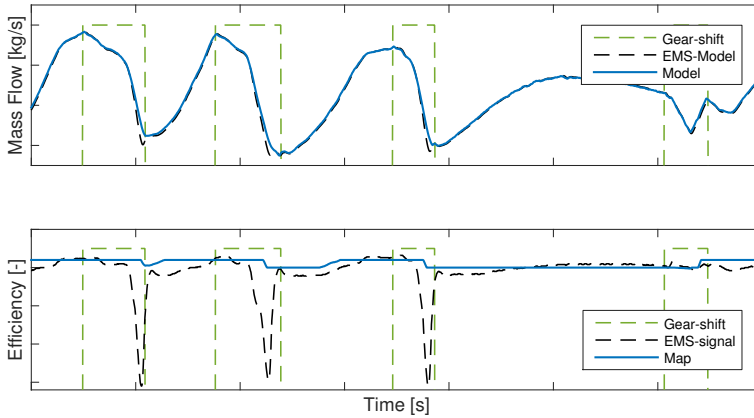


**Figure 4.4:** Air mass flow validation plot, for model using mapped volumetric efficiency and corrected volumetric efficiency.

### Losses

The losses are validated against modelled EMS-signals using the same basic maps, and show an overall good fit. However, some discrepancy is found for the pumping losses, which leaves a slight offset of roughly  $A Nm$  in the total losses. With this as correction, the losses align better during gear-shifts as seen in Figure 4.5. The slight delay seen at the peaks during exhaust gas break can be traced to the filtration of the exhaust gas sensor signal. Since the offset is different for the two tested trucks it can only be used for simulation testing, whereas for final implementation it is more suitable to use the original EMS-functions, where the exhaust pressure is used unfiltered.

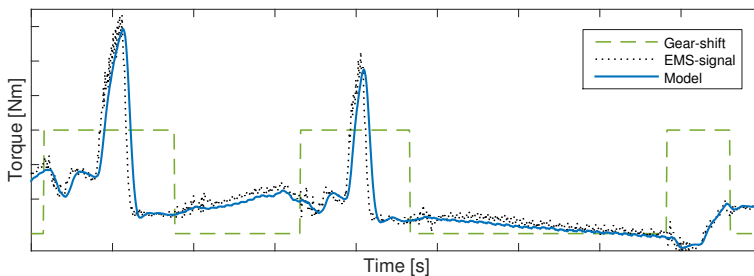


**Figure 4.5:** Total cylinder losses.

## Auxiliary Equipment

Apart from the losses in the cylinder, the torque consumption from the auxiliary devices needs to be taken into account. There are several systems powered by the engine, such as the cooling fan, air compressor, water pump, generator and air conditioning compressor. To model these components for the purpose of determining fuel injection during gear-shift, the same approach of using mapped data from torque calculations is applied.

However, not all units necessarily run at all times but are controlled by separate control systems that check reference signals for when to activate or at which load to operate. This makes predictable modelling a larger issue since the model would need to consider for instance brake pressure system refilling and when the driver wishes to activate air conditioning. Therefore they are here assumed to remain either deactivated or activated throughout the simulation depending on their state at the simulation initiation. This approach introduces a possible deviation in case any system activates or deactivates during the gear-shift. In Figure 4.6 it can be seen how total aggregate consumption varies over time. The air compressor is in this case not included in the model but would as seen add roughly  $B Nm$ .

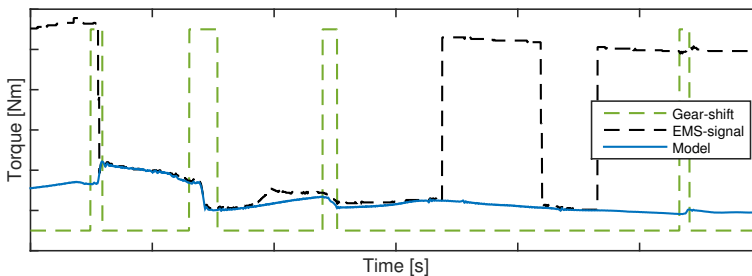


**Figure 4.6:** Auxiliary equipment torque consumption EMS-signal plotted with model where the air compressor is omitted.

The maximum possible deviation from the binary assumption above sums up to about  $C Nm$  if both air compressor and air conditioning suddenly activate during gear-shift for the tested engine configuration. If the assumption is taken further by fixating the otherwise speed dependent load, to stay constant during gear-shift the additional maximum possible deviation is about  $D Nm$ . That is if there is a gear-shift from the lowest engine speeds to the highest. The occurrence of maximum possible deviation in one gear-shift is therefore unlikely but would finally affect the exhaust temperature outcome which is explained further in Section 4.4.5.

#### 4.4.4 Fuel Mass Flow

Summing the total work from the cylinder the fuel mass flow can be calculated with Equation 2.32. Given the demanded torque and engine speed, a look-up table returns the desired amount of injected fuel at each stroke. This accounts for the engine's ability to produce work on the piston from the chemical energy in the fuel.

The actual fuel injection is based on the same map, but as in before mentioned cases, there are more complex EMS-functions to use that correct the mapped data to additional parameters, such as injection timing for instance. However, using the basic map as seen in the validation plot in Figure 4.7 gives a good fit for gear-shifts and deviates only slightly at the high load where injection timing is unmatched.

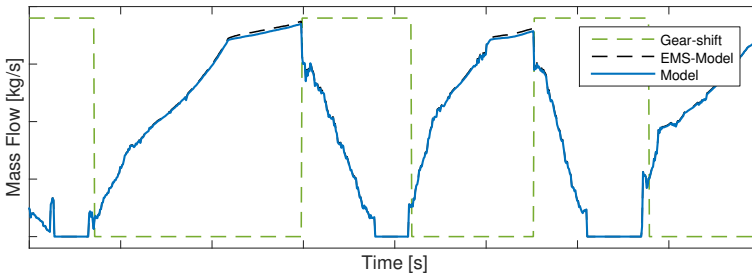


Figure 4.7: Fuel injection model

#### 4.4.5 Exhaust Gas Temperature

The model for exhaust gas temperature uses Equation 2.35, where the parameter  $k_T$  is fitted to experimental data using a least square method that creates a surface based on fuel flow and engine speed.

An improvement made to the linear model for  $k_T$  is to split the load range into high and low loads respectively, which results in two separate linear regions. This is required since the temperature model needs to operate at a wide range of loads. To design these linear regions one must first decide which points to include in the least square estimation for each region and second where to draw the line for which amount of fuel to be considered as high or low load. These decisions can be seen as tuning choices and result in two sets of the parameters  $k_e$ ,  $k_N$  and  $k_f$ .

The plots in Figure 4.8 are 2D projections of the original 3D space. The left plot shows how the linear regions are fitted with the calculated data points in the fuel flow/parameter-plane (x/z-plane) for a certain segment of engine speed. The right plot shows only high loads in the engine speed/parameter-plane (y/z-plane), which corresponds to about the right 2/3 part of the left plot. For the

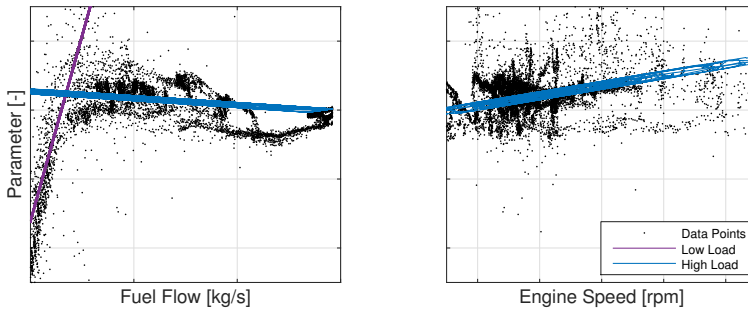


**Figure 4.8:** 2D-plots of the linear region separation. To the left the third dimension engine speed is fixed around one certain speed for visualisation. The dividing point is chosen to where the low and high load regions intersect. To the right, only the high load points are shown.

validation against the corresponding EMS model seen in Figure 4.9. It can be seen that the linear temperature model in some high load points deviates almost  $\pm 10\%$ , but overall has a good fit. It is clear that the simplification of linearising the temperature behaviour will generate wrong estimations at some points, and the impact of this is to be investigated in the simulation evaluation in Section 5.2.3.

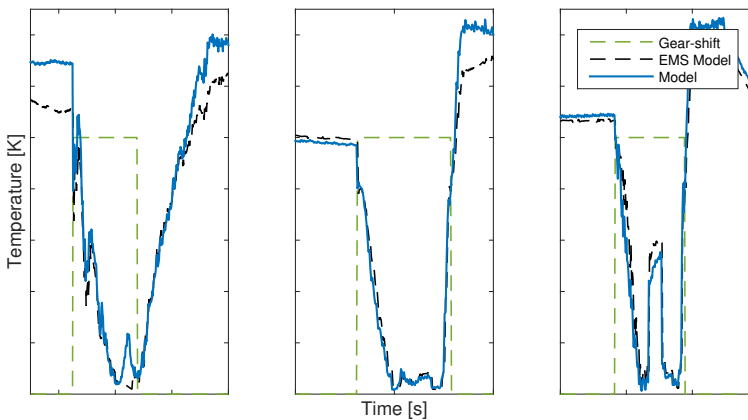


**Figure 4.9:** Exhaust temperature time plot for three gear-shift cases.

### 4.4.6 Exhaust Manifold

Similar to the intake manifold, the exhaust manifold is modelled as an dynamic isothermal control volume. The exhaust mass flow out of the engine as inflow and a mass flow model for the turbocharger as outflow constitute the filling and emptying dynamics of the manifold. As manifold temperature, the modelled exhaust temperature is assumed to be representative for the entire volume and not change during the transport through it. This simplification neglects the temperature dynamics in the manifold completely, and the main reason for this is that it is difficult to validate such dynamics without proper sensors.

### 4.4.7 Turbocharger

The turbocharger model is divided into the three main components; turbine, compressor and connecting shaft. The turbine and compressor have static models that connect through the dynamic power balance of the shaft given by Equation 2.20. The components powers are modelled using equations 2.23-2.26, where the mass flow models are described in the sections below.

For the efficiencies of both components there exists models and lookup tables that work well for steady state operating points. However, in this implementation, the compressor efficiency  $\eta_c$  as well as the turbine efficiency  $\eta_t$  has been assumed constant to act as a tuning parameter in the simulations. These must be tuned in accordance with each other since both have similar effects on the overall performance of the simulations.

#### Compressor

Here a compressor map is used to extract the mass flow given the pressure ratio over the compressor and the turbocharger speed from the shaft dynamics. This look-up table is originally stored in the EMS to interpolate a turbocharger speed given pressure ratio and mass flow since the latter can be either measured or modelled from other live measurements. In this case the table has to be inverted in order to extract the mass flow.

#### Turbine

The turbine mass flow is modelled using a non physical model suggested in Eriksen and Nielsen [2014] based solely on pressure ratio  $\Pi_t$ , as follows in Equation 4.2.

$$\dot{m}_t = k_1 \sqrt{1 - \Pi_t^{k_2}} \quad (4.2)$$

Where parameters  $k_1$  and  $k_2$  initially can be fitted using a least square method. Here the Matlab function *lscurvefit* is used to fit the parameters to the exhaust mass flow and pressure ratio between exhaust manifold pressure and ambient pressure. To keep in mind here is that this model does not by itself consider the effect of the exhaust gas brake, which is further explained in the Section 4.4.8.

The parametrization does therefore not consider data points when the exhaust gas brake is active, which yields the curve shown in Figure 4.10. Some necessary adjustments to this parametrization are addressed in Section 4.5.

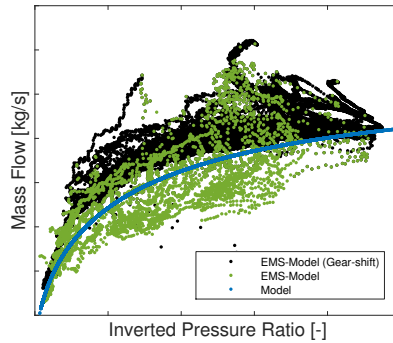


**Figure 4.10:** Model of turbine mass flow based on pressure ratio. The model follows the green points that account for gear-shifts when the exhaust gas brake is not active. The black points correspond to loads over a certain level to show the distribution of normal operating points.

#### 4.4.8 Exhaust Gas Brake

There are two main issues in implementing the exhaust gas brake in the simulation model. The first is the complex relation between demanded actuation and actual actuation, which depends on the component characteristics and current operating conditions. The second issue is that of modelling predictably. In order to model the actuation during simulation it has to be known what level of actuation will be demanded, which essentially depends on how fast the GMS requests to perform the gear-shift.

That being stated, to properly model the turbine mass flow during exhaust gas brake, it is necessary to model the actual pressure ratio over the turbine. The exhaust gas brake will, when closing, raise the exhaust back pressure and consequently bring down the pressure ratio over the turbine, which lowers the flow past it. In Figure 4.11, this is illustrated in a plot similar to the one in Figure 4.10. Now, since the turbine mass flow model uses the ratio between ambient and exhaust manifold the raising of exhaust manifold pressure would yield a higher flow (which can be imagined if the pressure ratio in Figure 4.11 were to be translated to mass flow using the model in Figure 4.10).

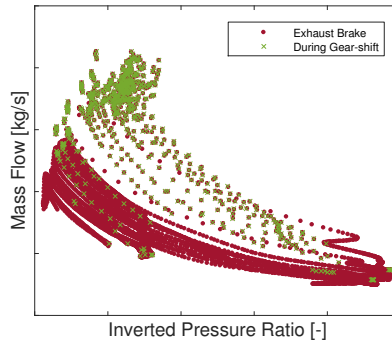


**Figure 4.11:** Turbine mass flow based on pressure ratio during exhaust gas brake. The green crosses indicate actuation during gear-shifts. Some margin of error in finding the correct points is expected due to difficulties in sorting out the short actuation impulses.

Currently, there is no model implemented to remedy this and the effects of completely disregarding the exhaust gas brake are investigated in the simulation validations in Section 4.5.1. However, it was tested to adjust the mass flow model under the assumption that the requested brake level were known. As presented in Section 2.2.5, it is possible to model the mass flow in a throttling mechanism through equations 2.14-2.17. First, during these tests a model based on a second order filter is applied to the recorded pressure demand signal. This yields an exhaust manifold pressure behaviour similar to the measured one, with deviations due to afore mentioned reasons. Treating this as the demanded pressure signal, possible delays and irregularities are omitted. This new demand signal can then be used to find a model for the effective open area  $A_{eff}$  as a function of the demanded pressure.

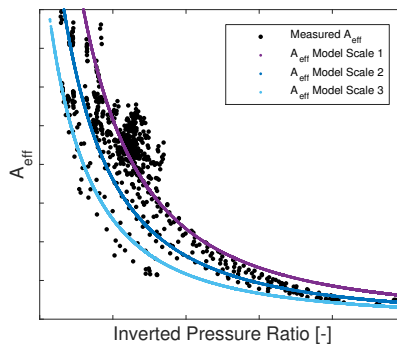


**Figure 4.12:** Exhaust gas brake effective opening area.

The model in Figure 4.12 is determined by postulating a curve shape and determining its parameters using a curve fitting tool in Matlab with calculated  $A_{eff}$ . With this, the turbine mass flow can be assumed equal to the exhaust gas brake flow during its activation. A probably necessary adjustment to this model in a future implementation is to scale the curve to current conditions with one of the parameters. This is illustrated with three differently scaled curves in Figure 4.12, this is however not fully investigated.

#### 4.4.9 Waste Gate

The waste gate will also affect the turbine mass flow during activation and should therefore be taken into account. When active, the pressure in the exhaust manifold will not only feed the turbine mass flow but also push a mass flow leakage through the waste gate and thereby decrease the power to the turbine. To model the waste gate Equation 2.14 is used. The modelling issues are here similar to those mentioned for the exhaust gas brake. The delay in the actuation is modelled with a second order filter applied to the signal of the actuator current level and an assumed proportionality between current and opened orifice area. Since the waste gate is set to open at a certain level below maximum torque this parameter can be used to model the current signal.

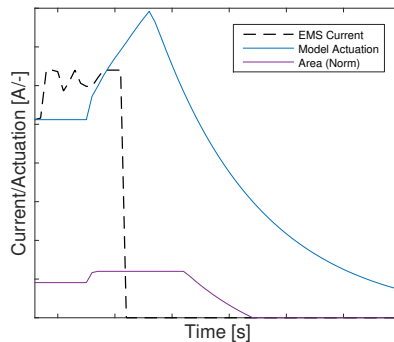


**Figure 4.13:** Model of waste gate actuation, where the opening area is normalized to fit the plot. Here the waste gate starts partly open, reaches the fully open state and closes as the signal drops below the limit value.

## 4.5 Simulation Model

The principle of the simulation itself is based on a filling and emptying cycle that sequentially steps through the dynamics of the engine gas path. Explained in Figure 4.14 is the the loop performed once each time increment and repeated until the gear-shift ends.

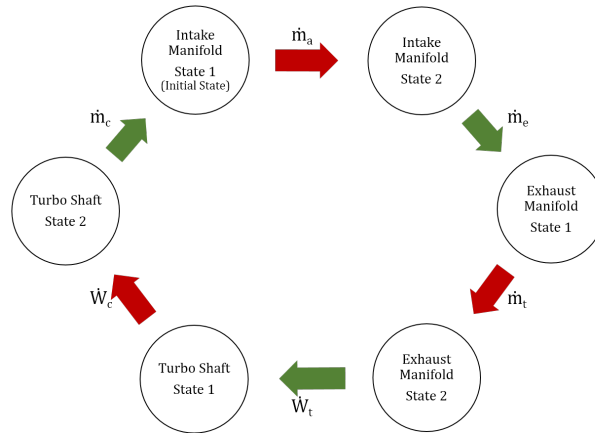


**Figure 4.14:** Simulation strategy, where the circles represent states of control volumes that are determined by the filling or emptying through the restrictions represented by the green or red arrows respectively.

By starting at the given initial conditions for the intake manifold and using it for calculating the engine airflow, the second intake manifold state is found. Using that state and the initial exhaust manifold state, the combustion can be calculated in terms of exhaust temperature and exhaust mass flow. Further applying the same approach for the following control volumes and restrictions the cycle is completed and can be repeated for as long as reference signals are available.

The simulation model is initially developed in a Matlab script where all states and flows are calculated and then looped through the given reference signals. In this way, the simulation results can be plotted against the data sets gathered in the experiments. The pressure dynamics in both exhaust and intake manifold are here compared to the filtered sensor signals, while the turbocharger speed dynamics is compared to an EMS-model based on the compressor map.

### 4.5.1 Sub Model Validation and Tuning

The first step of validating the simulation model is to use the measured speed and actual torque demand signals as inputs for several gear-shifts of different types. An example of a simulated gear-shift is shown in Figure 4.15, where the pressure and turbo dynamics can be analysed together with sub models and reference signals. From these types of plots it is possible to draw conclusions on the sub models actual performances to tune them appropriately. Important to

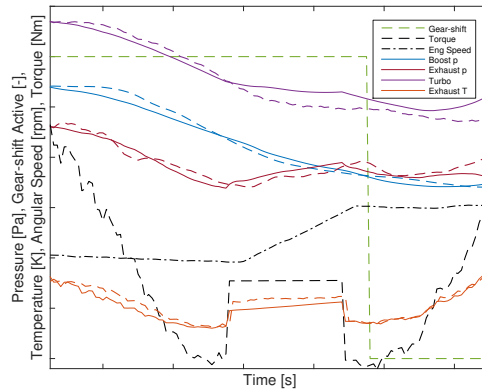


**Figure 4.15:** Example of a simulation plot where the sub model signals (solid lines) are plotted against measured signals (dashed lines). Except for the pressures, the rest of the signals are scaled to fit the plot.

consider is that tuning of parameters must be valid for all cases or rely on interchangeable or adaptive schemes that suit the actual case. These of course can only be based on information known before simulation initiation.

### Exhaust Temperature

Following the exhaust pressure signal in Figure 4.16, the impact of exhaust temperature rise can be noticed in the synchronization phase. In order to fit the non-dynamic model to the exhaust manifold pressure dynamics a time delay of  $10ms$  is added to the temperature model, which physically accounts for some part of the inertia in the manifold volume.

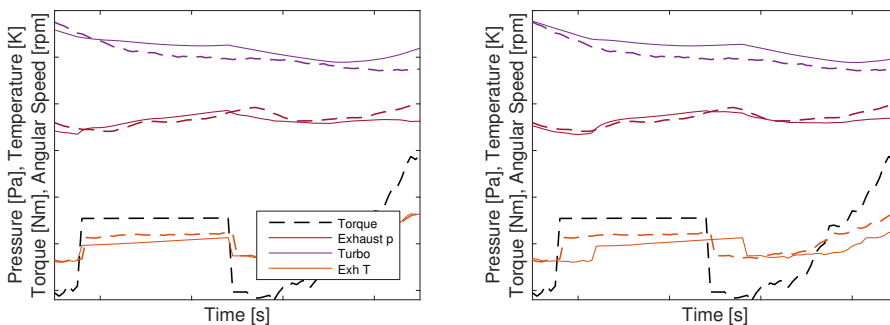


**Figure 4.16:** Effects of including a delay to the exhaust temperature model. The left plot shows the initial offset in the exhaust pressure and the right shows the adjustment. Dashed lines represent measurement references.

### Exhaust Gas Brake and Waste Gate

As can be seen in the two plots to the left in Figure 4.17, the exhaust manifold pressure does not follow the measurement signal at all in the sync phase. The modelled signal is however more correct in terms of pressure ratio over the turbine, but still too high since the ratio should be close to one. Though without any exhaust gas brake model, the simulation fails to represent a small but noticeable drop in turbocharger speed and thereby boost pressure.

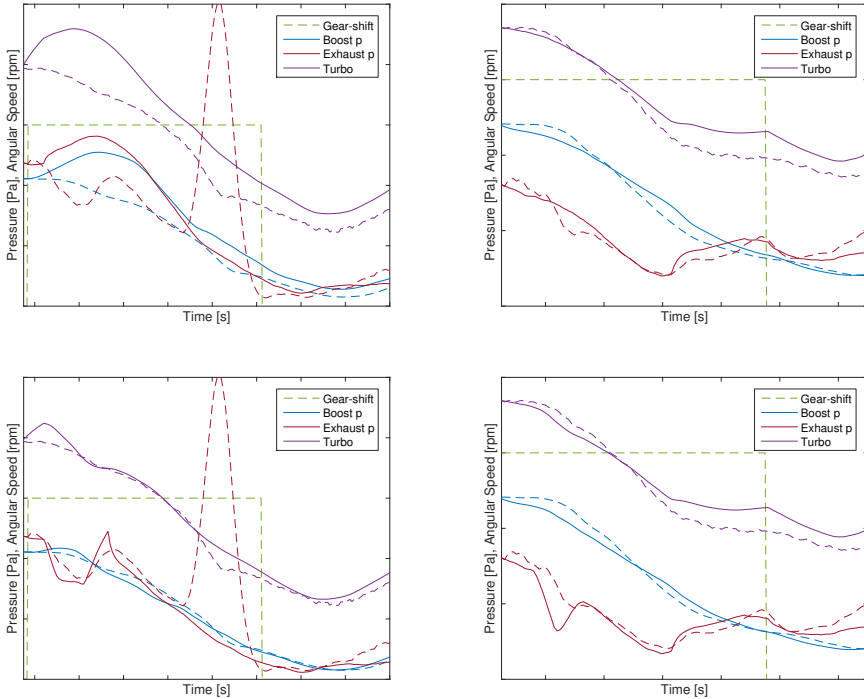


**Figure 4.17:** Effects of including the waste gate model into the simulation for an up-shift to the left and a down-shift to the right. Above are simulations without the waste gate model and below with it included. Dashed lines represent measurement references.

The exhaust pressure curve also gives away the effects of the waste gate actuation, which is seen as a small drop in both the left and right case in Figure 4.17. In the beginning of the down ramp this temporary drop can be seen that is due to a short impulsive opening of the waste gate when suddenly dropping the torque demand. Including the waste gate model yields the lower plots, where the turbocharger speed and boost pressure have been stabilised as well. The difficulties with modelling the waste gate can be identified by noticing the irregular behaviour of the exhaust pressure in the resulting plots. The simulation results and overall performance of waste gate model usage are presented in Section 5.2.

### Turbine Mass Flow Parameter

In the implementation of the simulation strategy the turbine flow is determined before the emptying of the manifold when the pressure is temporarily at a high state, see Section 4.5 and Figure 4.14. This means that the factorial parameter  $k_1$  needs to be considerably lower than when parametrizing with static data points to yield the correct pressure dynamics. The solution to this is to fit the parameter to initial conditions when initiating the simulation. This includes the effects of the waste gate in case it is active at initiation.

A further adaptation that was found necessary to implement is to adjust the model for speed dependency. One theory presented in Eriksson and Nielsen [2014] suggests adding a speed dependent stagnation pressure, although here a speed dependent offset added to the factorial parameter  $k_1$  has been found to amend the issue. The improving effects can be seen in the right plot in Figure 4.18.

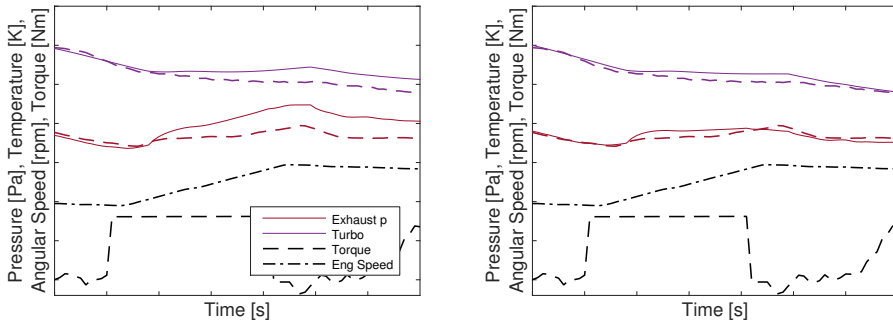


**Figure 4.18:** Improving effects (right plot) of including a speed dependent offset to the parameter  $k_1$  in the turbine mass flow model. Dashed lines represent measurement references.

### Compressor and Turbine Efficiencies

The efficiencies of compressor and turbine have been used as tuning parameters to adjust the dynamic behaviour. Essentially, this either gives overall higher or lower pressure values due to higher or lower turbocharger speeds. To tune these values, simulations for several gear-shifts were performed and compared. For both, suitable efficiency values lie around  $0.7 \pm 0.05$ .

#### 4.5.2 Simulation with Reference Input Model

The second step is to include the reference input model. This adds an uncertainty since much of the data used in the original ramp adaptations are not available to the reference input model. The discrepancies shown in Figure 4.2, which for some cases are larger, constitute a major contribution to estimation errors. A complete simulation using these modelled reference inputs is shown in Figure

4.19, were the results at each engine speed for one gear-shift are plotted together. As the purple speed line for  $1500rpm$  matches the real target speed, it is also the purple boost pressure curve that will represent the final result at the descending flank of the dashed gear-shift line. In other cases, interpolation of the boost pressures along the gear-shift line given a target speed would yield the final boost pressure.

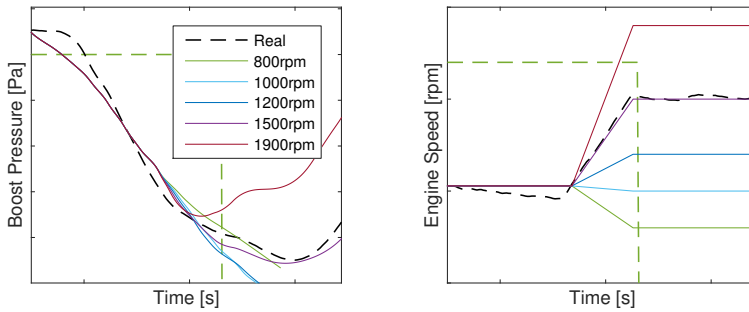


**Figure 4.19:** Complete simulation of the five engine speeds, with boost pressure results to the left and their corresponding engine speeds to the right. Dashed lines represent measurement references.

At this stage however, it is more difficult to tune sub models since qualitative examinations get more complicated as seen in Figure 4.19. It is here easier to turn to quantitative methods, both for analytical reasons and visualisation. To do this, the five final boost pressures at the end of the gear-shift are picked out of the simulation and interpolated using the correct engine speed. These are also interesting to compare with the same results for the simulations with measured inputs. These are presented as statistical results in the simulation results in Section 5.2.



# 5

---

## Results and Discussion

This chapter presents all results from the thesis. Starting with the analysed statistical results from the experiments and continuing with the results from the modelling and implementation thereof, to finish with the performance and tolerance analysis of the implementation.

### 5.1 Experiments

Here the statistical results of the experiments are presented. In order to sort out statistical data from gear-shifts according to certain parameters a script developed to go through all experimental data was used. From this several parameters were extracted to be plotted for analysis out of which the few most interesting are presented here. In the plots, the points each represent a gear-shift, where colours and markers indicate how many gears were shifted.

The gear-shifts were sorted out to represent high load and critical situations which are the most relevant ones. To do this, smoke limited gear-shifts were picked. As mentioned in Chapter 3, there were some deviations possibly affecting the data collection that one should be aware of when looking at the plots. Especially that down-shifts at high loads are much fewer, which makes statistical confidence lower, and also that the recordings with the truck Bolsena were recorded with an unintended waste gate actuation, which is probable to have affected the boost pressure behaviour.

### 5.1.1 Impact on Total Shift Time

As stated early in the report the boost pressure affects the torque response, which for gear-shifts has impact on the time to return to demanded torque. To show this, the final boost pressure (right before on-ramping) has been plotted against the total time of the gear-shift (when demanded torque is retained) in Figure 5.1. The four plots present results for the two tested truck configurations and up and down-shifts respectively. Clearly shown for all cases, is that a gear-shift takes longer time to perform if the boost pressure is lower.

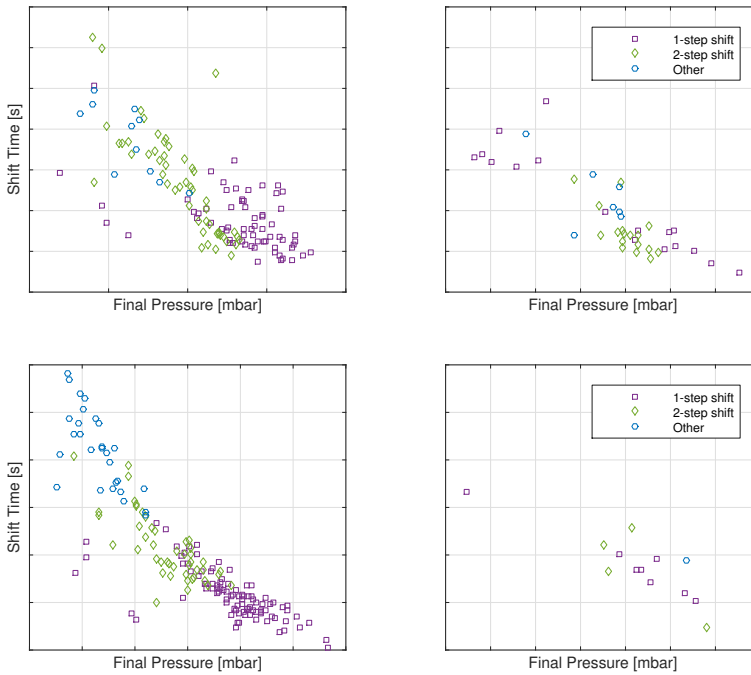


**Figure 5.1:** Total shift time plotted against final pressure for up-shifts (left) and down-shifts (right) for Clint (upper) and Bolsena (lower) respectively.

### 5.1.2 Boost Pressure Drop

To examine reasons for the pressure drop several collected parameters were plotted against it. Below follows results of two examples of chosen parameters.

#### Initial Pressure

The following four plots shown in Figure 5.2 show the drop in boost pressure plotted against the pressure at the beginning of the gear-shift in the same layout as before. Notable here is the linear dependence of the initial pressure. Although the down-shifts have much less recorded data points, especially for the lighter truck, a linear dependence is likely. From a practical point of view, this means that given the initial pressure it is possible to, within a certain confidence interval, predict the final boost pressure.

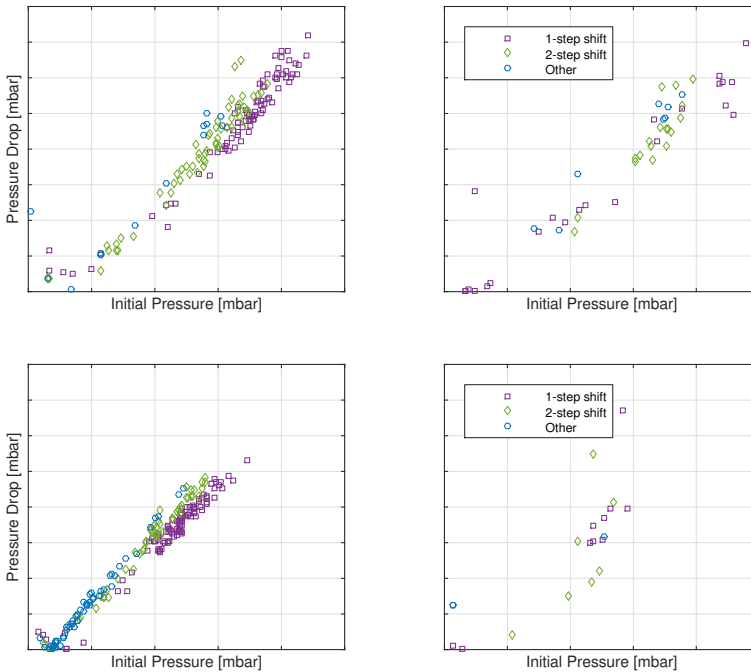


**Figure 5.2:** Pressure drop plotted against initial pressure for up-shifts (left) and down-shifts (right) for Clint (upper) and Bolsena (lower) respectively.

## Shift Time

In the second set of plots shown in Figure 5.3 the same boost pressure drop is plotted against the time until the on-ramp, which is not to be confused with the total gear-shift time. Here the relation is less obvious, thereby stating that the time a gear-shift takes to perform is not directly affecting how much the pressure drops. However, the distribution of markers indicate that number of shifted steps is related to both the gear-shift time and pressure drop. Since the ramping time of engine speed depends on both strategy and final engine speed, i.e. how many steps are to be shifted this result is expected.

Also to be kept in mind while reviewing these results is that many of the parameters are strongly interconnected, for instance that the strategy for selecting gears depend on the situation. As can be seen in Figure 5.3 it is natural for the system to perform smaller shifting steps if the load is high and thus also the boost pressure, which as seen in Figure 5.2, leads to a larger pressure drop.

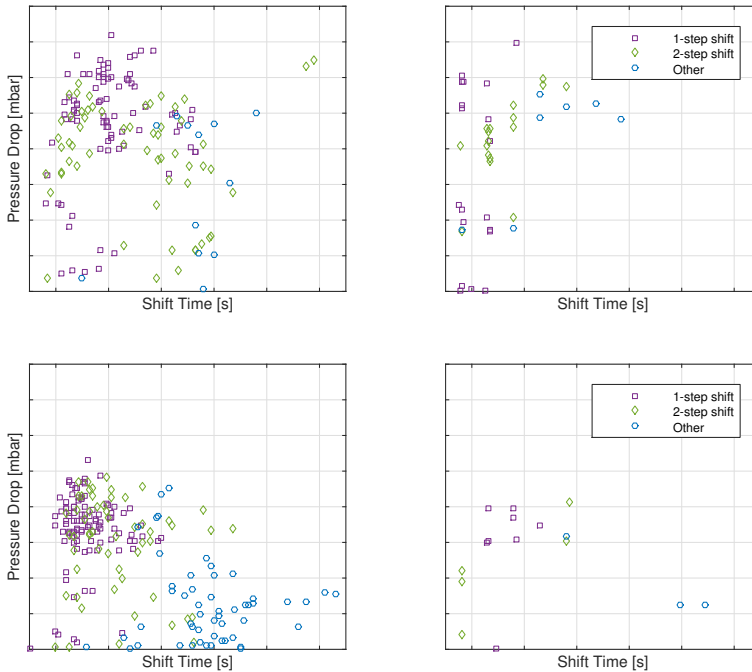


**Figure 5.3:** Pressure drop plotted against shift time for up-shifts (left) and down-shifts (right) for Clint (upper) and Bolsena (lower) respectively.

## 5.2 Simulation Results

Here the results from the simulations are presented in a statistical sense. Several time segments during gear-shifts are sorted out from the data sets acquired in the experiments by the same method as when presenting experimental results. This also means that only high load gear-shifts have been selected. Similarly to when manually picking out gear-shifts, the measured data is used to compare simulation results. By calculating the actual pressure drop and comparing it to the simulated pressure drop, it is possible to quantitatively assess the performance of multiple simulations in one plot.

This section aims to present a systematic evaluation of the simulation model performance before final implementation, which includes evaluation in terms of robustness based on identified sources of error that could affect its performance. Later on, this can be used as a basis for performance tuning and helps diagnosing possible errors in the final implementation.

There are several possible deviations that might affect the outcome of a model. In general, these are either input errors from for instance sensors or modelling uncertainties such as simplifications and faulty assumptions. This model relies on input data for a few initial conditions such as intake and exhaust manifold pressures and temperatures, turbocharger speed, demanded torque and engine speed. In Section 5.2.5, it is investigated what impact deviations in these inputs have on the model output, i.e. the sensitivity to deviations in the input parameters. As to the modelling, some main issues have been discussed already, and are subject of the performance analysis in Section 5.2.2.

### 5.2.1 Evaluation Method

It is important to be aware of how the chosen evaluation method works, since itself can alter the resulting outcome. This needs to be taken into account for both measured reference inputs and when using modelled reference inputs.

As seen in the simulation plots, for instance the example plot in Figure 4.15, there is a point where the boost pressure intersects the gear-shift descending flank. This is where the boost pressure is interpreted as final before the engine starts to deliver torque again. As also seen is that the boost pressure can continue to drop after this, which means that this chosen point is not always perfectly representative for the purpose of this model.

What more to be aware of is that the method, if seen as a method of evaluating the performance of the model, does not consider the overall performance but only the fit at a certain point of the simulation. The result is thereby presented independently of how well the model actually follows the measured trace. A bad simulation could still produce a good result if the model intersects the actual value at the correct point. This means that tuning parameters using these more quantitative methods has the drawback of not being able to ensure that the entire model behaviour improves, and could turn out to just tune this intersection point

closer to the chosen evaluation point. It can however be discussed how relevant trace following is, since the sought result is only a final boost pressure value.

## 5.2.2 Model Performance

Initially, the simulations using the measured inputs are presented in Figure 5.4. These results are considered as a best case scenario and will serve as comparison basis for the following sensitivity analyses. It can be seen that down-shifts are better estimated than up-shifts, which not always are estimated within the limits observed from the experimental results. As a measure of the simulation precision the RMS (root-mean-square) deviations are calculated and presented as a summary of all tested cases in Table 5.1.

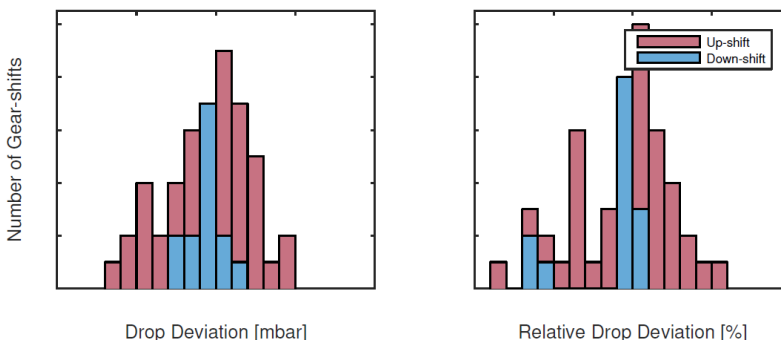


**Figure 5.4:** Histogram of simulation results in terms of deviation distribution using measured reference inputs.

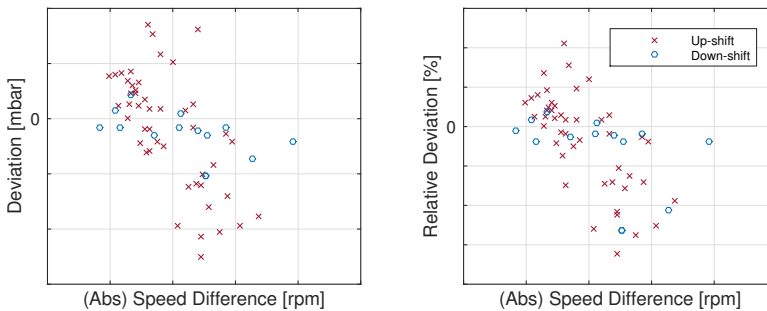


**Figure 5.5:** Simulation deviations dependence of engine speed difference.

Although the down-shifts are fewer, it is clear that their estimation accuracy is far better than for up-shifts. The reason for this is not fully investigated, but might be connected to the exclusion of the exhaust gas brake model. Supporting this theory is the fact that it was also identified that the deviations hide a dependency of speed difference, which affects the exhaust gas brake usage. However, there is

a subtle speed dependency for down-shifts as well. This can be seen in Figure 5.5, where the deviations are plotted against absolute speed difference. The difference in speed also correlates to how many gears are shifted.

### Waste Gate

As the waste gate model has some clear flaws due to modelling complications, it is interesting to study what the final effects to the estimation are when disregarding the waste gate. These simulation results are plotted in Figure 5.6.

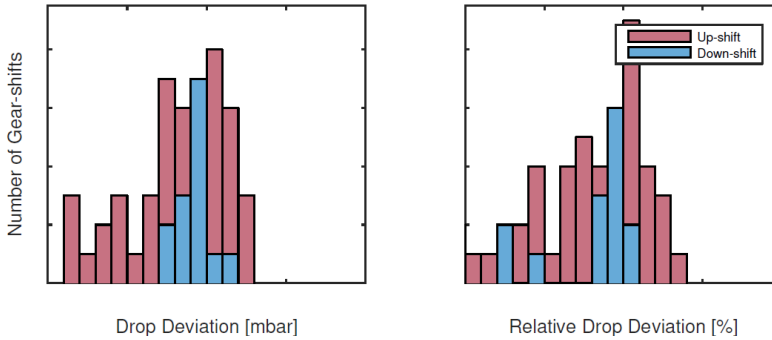


**Figure 5.6:** Histogram of simulation results in terms of deviation distribution using measured reference inputs and disregarding the waste gate model.

It can be deduced that excluding the waste gate has a slight effect of underestimating the pressure drop, thus overestimating the boost pressure, which is reasonable since bypassing exhaust gas past the turbine lowers the power to the system. Furthermore, the down-shifts continue to be more accurately estimated and the same speed dependency seen in Figure 5.5 is still there.

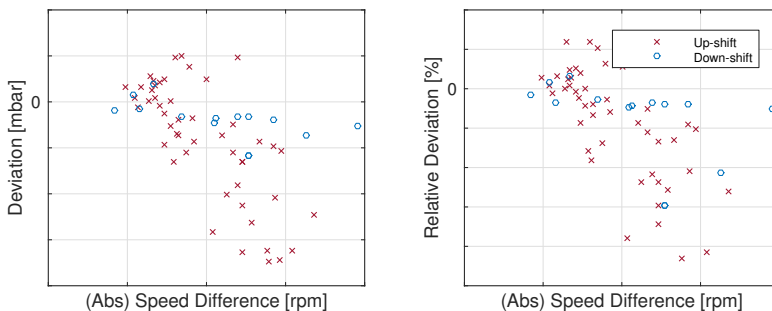


**Figure 5.7:** Simulation deviations dependence of engine speed difference when disregarding the waste gate model.

### Modelled Reference Inputs

It can be assumed that the reference input modelling uncertainty due to limited gear-shift information is source to deviations in the final output. By interpolating the final pressure the results can be plotted in the same manner as before to see what general effects these modelling uncertainties may have. In this case  $\eta_c$  and  $\eta_t$  were lowered in order to center all points around zero, which indicates that these simulations tend to underestimate the pressure drop (and overestimating the boost pressure). In figure 5.9 and 5.8 results are presented.

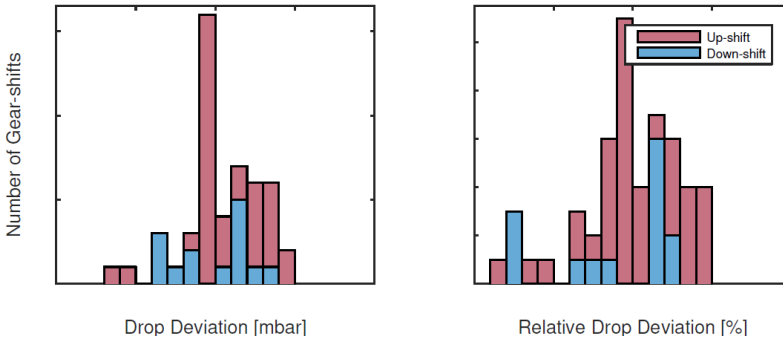


**Figure 5.8:** Histogram of simulation results in terms of deviation distribution using modelled reference inputs.

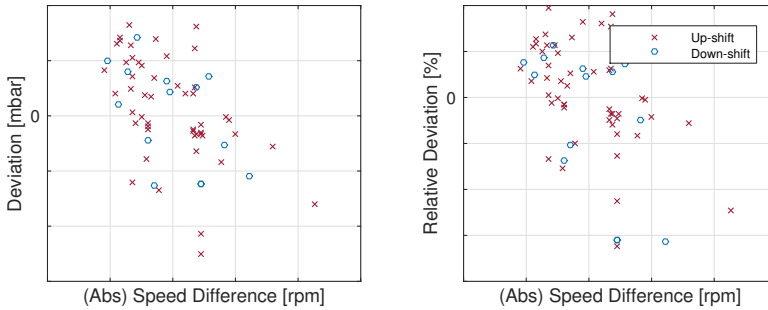


**Figure 5.9:** Simulation deviations dependence of engine speed difference using modelled reference inputs.

Surprisingly, these results indicate that simulations with modelled input references return slightly better up-shift estimations but far worse down-shift estimations.

### Modelled Reference Inputs Without Waste Gate

For sake of completion the two latter test were combined to see if the waste gate model still has the same impact on the modelled reference inputs. These results are presented in figure 5.9 and 5.8. Here, there is less impact of excluding the waste gate than when using the measured signals as inputs.

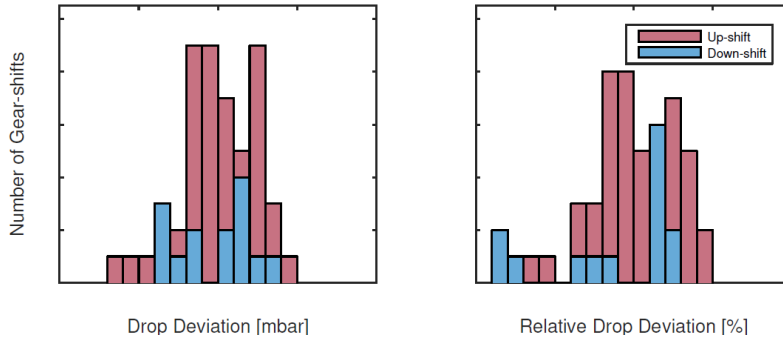


**Figure 5.10:** Histogram of simulation results in terms of deviation distribution using measured reference inputs and disregarding the waste gate model.

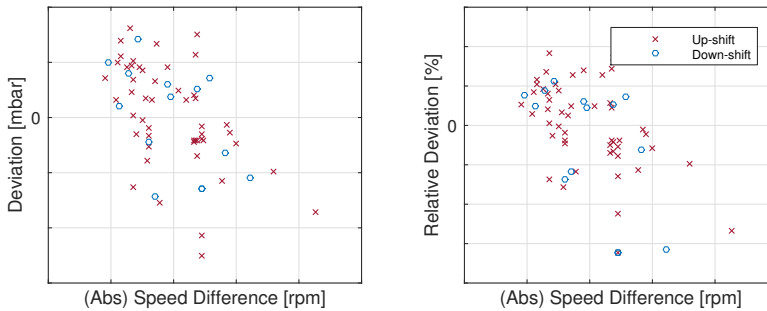


**Figure 5.11:** Simulation deviations dependence of engine speed difference using modelled reference inputs and disregarding the waste gate model.

**Table 5.1:** Summary of results in terms of RMS deviations of boost pressure drop for simulation cases, for up-shifts (US) and down-shifts (DS) respectively.

Simulation	RMSD US	RMSD DS
Measurement Inputs with WG	~100mbar	~50mbar
Measurement Inputs without WG	~150mbar	~50mbar
Modelled Inputs with WG	~100mbar	~100mbar
Modelled Inputs without WG	~100mbar	~100mbar

### 5.2.3 Sensitivity to Modelling Inaccuracies

As identified in the modelling chapter in Section 4.4.5 the fit of the linear exhaust temperature model is not very good and is likely to produce deviations in the simulations. It is therefore very interesting to investigate how much influence this modelling error might have compared to a nominal case, here set to the case with measurement inputs without waste gate.

Deducted from the theory and the plots of the linear model, a possible error has the most influence for higher load regions, since the temperature is based on amount of fuel injected. Temperature deviations during the entire gear-shift are therefore tested for several gear-shifts and compared to their corresponding nominal case. The method and resulting outputs is illustrated for one downwards gear-shift in Figure 5.12. The total results are presented in Table 5.2 where the RMS deviations are summarized.

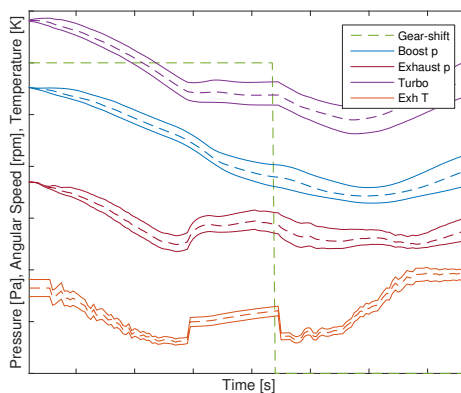


**Figure 5.12:** Example of simulation sensitivity to temperature deviations. Dashed lines are nominal values and the solid lines are positive and negative deviations from their respective nominal value.

**Table 5.2:** Results for temperature offset with resulting RMS deviation of boost pressure drop from nominal result for up-shifts (US) and down-shifts (DS) respectively. A negative pressure drop RMS deviation means that the boost pressure is underestimated and vice versa.

Simulation	RMSD US	RMSD DS
Worst Case	~+125mbar	~+125mbar
	~-100mbar	~-100mbar
Realistic Case	~+50mbar	~+50mbar
	~-50mbar	~-50mbar

### Torque Demand Deviations

Deviations in torque demand influences fuel injection and thereby the exhaust temperature estimation. The modelling simplification of assuming the auxiliary systems to maintain their initial value constant during a gear-shift was assessed to a worst case scenario, which would then include the change in engine speed in a maximum range gear-shift. In the same way as before, simulations with the deviations are compared to the nominal case to see how they would affect the pressure drop estimation. Both the worst case deviation and a more likely deviation that could derive from other sources as well, such as badly constructed reference inputs, are tested and presented in Table 5.3.

**Table 5.3:** Results for torque demand offset with resulting RMS deviation of boost pressure drop from nominal result for up-shifts (US) and down-shifts (DS) respectively.

Simulation	RMSD US	RMSD DS
Worst Case	~+50mbar	~+50mbar
	~-25mbar	~-50mbar
Realistic Case	~+25mbar	~+25mbar
	~-25mbar	~-25mbar

### 5.2.4 Sensitivity to Parameter Changes and Calibration

The parametrized models are fitted to experimental data for one certain truck, in this case the 6-cylinder truck Clint. If not manually recalibrated for other engine configurations it is a possible source of deviation. As a measure of robustness, it is tested what deviation is inflicted to the nominal case of Clint if using parameters in the linear exhaust temperature model originally fitted to data from the 5-cylinder truck Bolsena. Results are shown in 5.4.

**Table 5.4:** Results for parameter changes in terms of RMS deviations of boost pressure drop for comparison cases, for up-shifts (US) and down-shifts (DS) respectively.

Comparison	RMSD US	RMSD DS
To Nominal Case	$\sim -25\text{mbar}$	$\sim -75\text{mbar}$
To Measured Result	$\sim 125\text{mbar}$	$\sim 50\text{mbar}$
Nominal to Measured Result	$\sim 150\text{mbar}$	$\sim 50\text{mbar}$

Remarkable here is that using the parameters fitted for Bolsena yields a better overall RMS deviation, than those fitted for the actual engine configuration. What can be deducted however is that the 5-cylinder truck parameters tend to estimate a lower temperature since the pressure drop deviation is negative. The most probable cause for the better fit is that the nominal case is slightly off center and would benefit from retuning the turbocharger efficiencies.

### Turbocharger Efficiencies

Mainly as a support for tuning it is interesting to see how changes of the turbocharger efficiencies  $\eta_c$  and  $\eta_t$  affect the output. As mentioned in the previous section, there might be room for optimization in setting these parameters. Below in Table 5.5 are results for upwards and downwards change in both parameters.

**Table 5.5:** Efficiency offsets with resulting RMS deviation of boost pressure drop from nominal case (NC) and measured result (MR) for up-shifts (US) and down-shifts (DS) respectively.

Case	Parameter	RMSD US	RMSD DS
NC	$\eta_c$	$\sim +50\text{mbar}$	$\sim +50\text{mbar}$
		$\sim -50\text{mbar}$	$\sim -50\text{mbar}$
	$\eta_t$	$\sim +50\text{mbar}$	$\sim +50\text{mbar}$
		$\sim -25\text{mbar}$	$\sim -25\text{mbar}$
MR	$\eta_c$	$\sim 150\text{mbar}$	$\sim 100\text{mbar}$
		$\sim 125\text{mbar}$	$\sim 50\text{mbar}$
	$\eta_t$	$\sim 150\text{mbar}$	$\sim 100\text{mbar}$
		$\sim 125\text{mbar}$	$\sim 50\text{mbar}$
Reference	-	$\sim 150\text{mbar}$	$\sim 50\text{mbar}$

As the table shows, the model is more sensitive to changes in the compressor efficiency  $\eta_c$ . Furthermore, it is shown that a decrease in either one of the parameters

would improve the deviation from the measured results when using nominal values.

### 5.2.5 Sensitivity to Input Deviations

Input sensitivity is tested by assuming reasonable deviations to sensors and EMS-signals. These deviations are summarized as offsets to initial conditions as seen in Table 5.6. Manifold sensors are considered to be relatively accurate within their usual operating range. The exhaust temperature input uses an EMS-model which when used as a turbine temperature is likely to deviate considerably depending on operating point, and specially in transient conditions. Its inaccuracy is therefore assumed relatively high. Likewise, the turbocharger speed is model based, and therefore this input inaccuracy is assumed high to account for sub optimal operating points.

Since the usage of modelled reference inputs is considered a quite sporadic source of error the following analyses are performed using simulations with measured reference inputs as nominal case. The resulting deviations are presented together with the tested offsets in Table 5.6.

**Table 5.6:** Initial parameter offsets with resulting RMS deviation of boost pressure drop from nominal result for up-shifts (US) and down-shifts (DS) respectively.

Input Parameter	RMSD US	RMSD DS
$p_{im}$	$\sim \mp 50 \text{ mbar}$	$\sim \mp 50 \text{ mbar}$
$p_{em}$	$\sim \pm 25 \text{ mbar}$	$\sim \pm 25 \text{ mbar}$
$T_{im}$	$\sim \mp 0 \text{ mbar}$	$\sim \mp 0 \text{ mbar}$
$T_{em}$	$\sim \pm 25 \text{ mbar}$	$\sim \pm 0 \text{ mbar}$
$\omega_{tc}$	$\sim +25 \text{ mbar}$	$\sim +25 \text{ mbar}$
$\omega_{tc}$	$\sim -0 \text{ mbar}$	$\sim -25 \text{ mbar}$

As can be deduced from the results is that a deviation in the boost pressure input would have largest impact on the result. At first glance this is not very surprising since the deviation is set to the parameter at which the result is evaluated. However, quite counter intuitively, a positive initial offset leads to a negative final deviation. On the other hand, this is exactly what was shown in the experimental results, that a higher initial boost pressure yields a higher drop, and thus a lower final boost pressure.

Furthermore, it can be seen that offsets to either the exhaust manifold pressure or temperature gives a larger pressure drop, which is also true for the turbocharger speed. This is reasonable since this means that the turbocharger will have more energy to keep the boost pressure up during the gear-shift.

### 5.3 Implementation in ECU for Vehicle Testing

As the next step of the implementation, the original Matlab code was implemented in Simulink to be code generated into C-code to be run in the ECU software. This part of the work was carried out by engineers at Scania parallel to finalizing the model evaluation due to shortage of time.

The following tests with the resulting implementation in the ECU of a heavy duty truck did however not turn out as originally planned during the time of this thesis. Initial test resulted in ECU-resets due to soaring computational load for engine speeds just above idling. The specific reason for this was not definitely established but is probably a result of time shortage while translating the Matlab code into executable ECU-code, since such environments are far stricter and more demanding in terms of robustness than PC-environments.

Further tests were carried out on ECU-hardware in simulated test environments on bench where the model module's used processing power was investigated. As a first indication of the current load it was estimated that the module accounted for almost 10% of the total calculation load for a certain partition. This is considered as a quite large load for a single module. It should however be kept in mind that the module in this condition had not been optimized in terms of computational efficiency and it can be assumed that the processor load with further work could be considerably reduced.

These ECU-tests did, during the time of thesis, not produce any results that were comparable to simulations carried out on PC.

### 5.4 Summary

The evaluation of the simulation results shows that the model using measured inputs estimates boost pressure drops within  $\sim 200\text{mbar}$  for the 95th percentile with RMS deviations of  $\sim 100\text{mbar}$  and  $\sim 50\text{mbar}$  for up-shifts and down-shifts respectively. The corresponding values when using modelled reference inputs, which must be used in further implementations, are  $\sim 200\text{mbar}$  for the 95th percentile with RMS deviations of  $\sim 100\text{mbar}$  and  $\sim 100\text{mbar}$  for up-shifts and down-shifts respectively. Concluding, this shows that the model is more than capable of returning values that are better estimated than when just looking at the experimental results. This is true for all cases, such as disregarding the waste gate model and using modelled reference input.

Plotting the deviations against speed difference, also interpreted as gear-shifting steps, a speed dependence in the deviations can be surmised. This results in higher deviations for larger speed differences. It is likely that for up-shifts this is connected to the exclusion of the exhaust gas brake since larger steps in engine speed demand more braking to reach target speed. This behaviour however is also seen in down-shift, and is enhanced as the modelled inputs are introduced. There might be more than one cause to this, and one further theory is that the

speed adaptation used for the turbine mass flow is sub optimal.

As can be deduced from all tested sensitivities is that deviations in several parts of the model have significant influence on the estimated boost pressure. Although none of the tested deviations even in their worst case are alone capable of making the model completely unusable, several added deviations could easily sum up to large errors. The sensitivities tested showed no obvious ranges of higher sensitivity for any tested parameter.

It should however be noted that some of the errors tested are already included in the performance, these are typically errors from modelling inaccuracies in EMS or the developed model. Such errors are not probable to develop over time and can thereby be assumed to in most cases sum up to a maximum deviation below  $\sim 200\text{mbar}$ , which is true for the 95th percentile of all cases.

Other inputs, such as from sensors ( $p_{im}$ ,  $p_{em}$ ,  $T_{im}$ ) could suffer from ageing and over time develop deviations according to the tested values. Ageing might also be a factor that affects parameter tuning for certain engine types over time. Furthermore it cannot be ruled out that some sensitivities or deviation behaviours differ between engine configurations or individual engines.



# 6

---

## Conclusions

The boost pressure behaviour during gear-shift has been investigated and documented. A predictive model of the engine dynamic gas path that estimates the boost pressure during gear-shifts has been developed and implemented in a vehicle ECU. Implementation has been done in a way that reduces the calibration burden to fit specific engine configurations with exception for some model parameters that need calibration. Simulations of the model on PC gives a good estimation of the final boost pressure compared to previously used values, but still has flaws that probably could be mended with further improvements. For instance, some of the simplifications used in the modelling work could probably be replaced with more complex models yielding more accurate results. Here one must bear in mind that model complexity often is a trade-off between performance and computational load.

A sensitivity analysis of the simulation model was carried out as well, where sensitivities of some modelling errors and input errors were tested. The conclusion to be made here is that there are several parameters that can have large influence on the model output. Of the sensors, the intake manifold pressure had the largest impact on the result. Also, possible modelling errors in the exhaust gas temperature had relatively large influence on the boost pressure outcome.

The tests in a heavy duty truck ECU however, did not yield satisfying results during the time of the thesis. Troubleshooting on test bench did however find probable causes to some of the errors and showed promising prospects of a functional implementation within a near future. Further results of the troubleshooting also indicated that the processor load of the current implementation was relatively high, which is why optimization of computational efficiency is suggested as a relevant part of the future work.

Although not being the main focus of the thesis, the development of the simulation model has yielded some indications on behaviours of the gas path dynamics. The experimental study has confirmed that there is a strong relation between initial pressure and pressure drop. Further it has confirmed that this drop has large influence on gear-shift time, which means all measures that conserve boost pressure will help reduce gear-shifting time, up to a certain point of course.

Since the model is general in terms of its physical modelling scheme it could, given further going reference inputs, serve to estimate the boost pressure during the rest of the gear-shift along the on-ramp. Furthermore, the simulation includes prediction of several parameters that could be useful in other, completely different purposes. These include the exhaust pressure and turbocharger speed dynamics as well as the static exhaust temperature and turbine mass flow. Some of these can be seen in the previously presented Figure 4.15. The model based approach allows for simple extraction of any sought parameter used in the calculations. These should however be investigated individually before usage to see if they meet desired accuracy levels for the intended purpose.

---

## Bibliography

- Per Andersson. *Air Charge Estimation in Turbocharged Spark Ignition Engines*. PhD thesis, Linköpings Universitet, December 2005. Cited on pages 4, 10, 13, and 26.
- Robert Bosch GmbH. *Bosch Automotive Handbook*. Bosch Handbooks series. Robert Bosch GmbH, 2007. Cited on page 3.
- Indranil Brahma, Yongsheng He, and Christopher J. Rutland. Improvement of neural network accuracy for engine simulations. In *SAE Technical Paper*. SAE International, 10 2003. Cited on page 4.
- Johan Bergström Jan Brugård. Modeling of a turbo charged spark ignited engine. Master's thesis, Linköpings Universitet, SE-581 83 Linköping, 1999. Cited on page 15.
- A. Chevalier, M. Muller, and E. Hendricks. On the validity of mean value engine models during transient operation. *SAE TRANSACTIONS*, 109:1571 – 1592, 2000. ISSN 0096736X. URL <https://login.e.bibl.liu.se/login?url=http://search.ebscohost.com/login.aspx?direct=true&db=edsbl&AN=RN104981781&site=eds-live>. Cited on pages 4 and 13.
- F. Chiara, Wang Junmin, C. Patil, Hsieh Ming-Feng, and Yan Fengjun. Development and experimental validation of a control-oriented diesel engine model for fuel consumption and brake torque predictions. *Mathematical and Computer Modelling of Dynamical Systems*, 17(3):261 – 277, 2011. Cited on pages 4 and 27.
- Per Darnfors and Alfred Johansson. Computationally efficient model for on-board simulation of heavy duty diesel engines. Master's thesis, Linköping University, SE-581 83 Linköping, 2012. Cited on page 4.
- Lars Eriksson and Lars Nielsen. *Modeling and control of drivelines*. John Wiley & Sons, second edition, 2014. Cited on pages 4, 12, 14, 16, 18, 26, 35, and 42.
- Jonas Fredriksson and Bo Egardt. Active engine control for gearshifting in auto-

- mated manual transmissions. *International Journal of Vehicle Design*, 32(3), 01 2003. Cited on page 4.
- José Galindo, José M. Lujan, Hector Climent, Carlos Guardiola, and Olivier Varnier. A new model for matching advanced boosting systems to automotive diesel engines. *SAE Int. J. Engines*, 7:131–144, 04 2014. Cited on page 4.
- L. Glielmo, L. Iannelli, V. Vacca, and F. Vasca. Gearshift control for automated manual transmissions. *IEEE/ASME Transactions on Mechatronics*, 11(1):17–26, 2006. ISSN 10834435. Cited on page 3.
- L. Guzzella and A. Amstutz. Control of diesel engines. *Control Systems, IEEE*, 18(5):53–71, Oct 1998. ISSN 1066-033X. doi: 10.1109/37.722253. Cited on page 4.
- Yongsheng He and Christopher J. Rutland. Modeling of a turbocharged di diesel engine using artificial neural networks. In *SAE Technical Paper*. SAE International, 10 2002. Cited on page 4.
- Elbert Hendricks, Alain Chevalier, Michael Jensen, Spencer C. Sorenson, Dave Trumpy, and Joe Asik. Modelling of the intake manifold filling dynamics. In *SAE Technical Paper*. SAE International, 02 1996. Cited on pages 4, 13, and 18.
- J.B. Heywood. *Internal Combustion Engine Fundamentals*. Automotive technology series. McGraw-Hill, 1988. ISBN 9780071004992. Cited on pages 3, 14, and 15.
- J.-P. Jensen, A.F. Kristensen, S.C. Sorenson, N. Houbak, and E. Hendricks. Mean value modeling of a small turbocharged diesel engine. In *SAE Technical Paper*. SAE International, 02 1991. Cited on page 18.
- Lennart Ljung and Torkel Glad. *Modellbygge och Simulering*. Studentlitteratur, second edition, 2004. Cited on pages 4 and 25.
- Michael J. Moran, Howard N. Shapiro, Daisie D. Boettner, and Margaret B. Bailey. *Principles of Engineering Thermodynamics*. John Wiley & Sons, 2011. ISBN 978-0-470-91801-2. Cited on page 11.
- F. Payri, E. Reyes, and J.R. Serrano. A model for load transients of turbocharged diesel engines. In *SAE Technical Paper*. SAE International, 03 1999. Cited on page 4.
- E. Perez, X. Blasco, S. Garcia-Nieto, and J. Sanchis. Diesel engine identification and predictive control using wiener and hammerstein models. In *Computer Aided Control System Design, 2006 IEEE International Conference on Control Applications, 2006 IEEE International Symposium on Intelligent Control, 2006 IEEE*, pages 2417–2423, Oct 2006. Cited on page 4.
- M. Pettersson and L. Nielsen. Gear shifting by engine control. volume 8, pages 495–507, May 2000. Cited on page 3.

- Frédéric Tschanz, Alois Amstutz, Christopher H. Onder, and Lino Guzzella. Feed-back control of particulate matter and nitrogen oxide emissions in diesel engines. *Control Engineering Practice*, 21(12):1809 – 1820, 2013. ISSN 0967-0661. Cited on page 19.
- Raymond Turin, Oguz Dagci, and Man-Feng Chang. Low-cost air estimation. *SAE Int. J. Engines*, 2:357–369, 04 2009. Cited on page 4.
- Abdullah Uzun. Air mass flow estimation of diesel engines using neural network. *Fuel*, 117(Part A):833 – 838, 2014. ISSN 0016-2361. Cited on page 4.
- Xiaofeng Yin and Anlin Ge. A dynamic model of engine using neural network description. In *Vehicle Electronics Conference, 2001. IVEC 2001. Proceedings of the IEEE International*, pages 109–114, 2001. Cited on page 4.
- Gianluca Zito and I.D. Landau. A methodology for identification of NARMAX models applied to diesel engines. *IFAC World Congress 2005, Prague, Czech Republic*, July 2005. Cited on page 4.





## Upphovsrätt

Detta dokument hålls tillgängligt på Internet — eller dess framtida ersättare — under 25 år från publiceringsdatum under förutsättning att inga extraordinära omständigheter uppstår.

Tillgång till dokumentet innebär tillstånd för var och en att läsa, ladda ner, skriva ut enstaka kopior för enskilt bruk och att använda det oförändrat för icke-kommersiell forskning och för undervisning. Överföring av upphovsrätten vid en senare tidpunkt kan inte upphäva detta tillstånd. All annan användning av dokumentet kräver upphovsmannens medgivande. För att garantera äktheten, säkerheten och tillgängligheten finns det lösningar av teknisk och administrativ art.

Upphovsmannens ideella rätt innefattar rätt att bli nämnd som upphovsman i den omfattning som god sed kräver vid användning av dokumentet på ovan beskrivna sätt samt skydd mot att dokumentet ändras eller presenteras i sådan form eller i sådant sammanhang som är kränkande för upphovsmannens litterära eller konstnärliga anseende eller egenart.

För ytterligare information om Linköping University Electronic Press se förlagets hemsida <http://www.ep.liu.se/>

## Copyright

The publishers will keep this document online on the Internet — or its possible replacement — for a period of 25 years from the date of publication barring exceptional circumstances.

The online availability of the document implies a permanent permission for anyone to read, to download, to print out single copies for his/her own use and to use it unchanged for any non-commercial research and educational purpose. Subsequent transfers of copyright cannot revoke this permission. All other uses of the document are conditional on the consent of the copyright owner. The publisher has taken technical and administrative measures to assure authenticity, security and accessibility.

According to intellectual property law the author has the right to be mentioned when his/her work is accessed as described above and to be protected against infringement.

For additional information about the Linköping University Electronic Press and its procedures for publication and for assurance of document integrity, please refer to its www home page: <http://www.ep.liu.se/>